

USING GISCIENCE METHODS TO ESTABLISH SPATIAL INFORMATION FOR  
PREHISTORIC SITES IN THE MALPASO VALLEY, ZACATECAS, MEXICO

THESIS

Presented to the Graduate Council of  
Texas State University-San Marcos  
in Partial Fulfillment  
of the Requirements

for the Degree

Master of SCIENCE

by

Ryan T. Schuermann, B.A.

San Marcos, Texas  
August, 2012

USING GISCIENCE METHODS TO ESTABLISH SPATIAL INFORMATION FOR  
PREHISTORIC SITES IN THE MALPASO VALLEY, ZACATECAS, MEXICO

Committee Members Approved:

---

Alberto Giordano, Chair

---

T. Edwin Chow

---

Charles D. Trombold

Approved:

---

J. Michael Willoughby  
Dean of the Graduate College

**COPYRIGHT**

by

Ryan Thomas Schuermann

2012

## **FAIR USE AND AUTHOR'S PERMISSION STATEMENT**

### **Fair Use**

This work is protected by the Copyright Laws of the United States (Public Law 94-553, section 107). Consistent with fair use as defined in the Copyright Laws, brief quotations from this material are allowed with proper acknowledgement. Use of this material for financial gain without the author's express written permission is not allowed.

### **Duplication Permission**

As the copyright holder of this work I, Ryan Thomas Schuermann, authorize duplication of this work, in whole or in part, for educational or scholarly purposes only.

## **ACKNOWLEDGEMENTS**

This work would not be possible without the guidance and direction from many people. I would like to thank the Department of Geography at Texas State University-San Marcos. A special thanks to my committee, Dr. Giordano, Dr. Chow, and Dr. Trombold for the indispensable help in guiding my thoughts to mold this paper into something tangible. I would like to thank Dr. Hagelman for helping me to lift my head out of the microcosm of space we archaeologists often focus on and look at the landscape surrounding it. A special thank you to Allison Glass-Smith, words cannot express how much you are appreciated. In addition, to my wife Ellie and my dog Chicha, for their understanding and patience while this paper came to fruition. Finally, to my parents, for decades of guidance and direction.

This manuscript was submitted on July 4th, 2012.

## TABLE OF CONTENTS

	<b>Page</b>
ACKNOWLEDGEMENTS .....	v
LIST OF FIGURES .....	viii
LIST OF TABLES .....	x
CHAPTER	
I. INTRODUCTION .....	1
II. PURPOSE .....	5
III. SITE AND SITUATION .....	9
IV. LITERATURE REVIEW .....	16
V. METHODOLOGY .....	26
Data Acquisition .....	26
1974 Survey Map .....	26
Digital Elevation Models .....	29
Other Imagery .....	34
GCP Selection Method .....	35
1974 Survey Map Assessment .....	35
Valleys .....	36
Peaks .....	37
Approach and Objectives .....	49
Process and Results .....	50
Geo-rectification .....	54
Validation .....	63
VI. RESULTS AND CONCLUSIONS .....	73
Results .....	73
Conclusions .....	81
Recommended tasks and additional work regarding improvements .....	83

Final Comments .....	84
APPENDIX A .....	86
APPENDIX B .....	90
LITERATURE CITED .....	91

## LIST OF FIGURES

<b>Figure</b>	<b>Page</b>
1. 1974 survey map.....	2
2. Mesoamerican northern frontier .....	10
3. Santiago-Lerma drainage basin.....	11
4. Middle Malpaso Valley, Zacatecas Mexico.....	12
5. Ruins of La Quemada, south side .....	13
6. Northern Mesoamerican socio-economic centers.....	14
7. Example of a vertical artifact in version 1 .....	31
8. Example of a lake as a sink in version 2.....	32
9. GDEMv2 example showing roadway and irregularities.....	33
10. 1974 survey map river channels compared to Landsat 5 and river network .....	37
11. Section of the topographic maps generated from the DEMs .....	40
12. Distribution of peaks used as control points.....	41
13. Subjective selection of optimal peak contour lines.....	42
14. Mean peak locations generated from interpolated peak sets .....	45
15. Distribution of standard peak distance of the DEM control point sets.....	46
16. Distribution of distance of the sets of INEGI DEM control points .....	47
17. Scatter Plot of the sets of INEGI DEM control points.....	48
18. 1974 survey map fit to display.....	51

19. Distribution of the 48 GCPs on the 1974 survey map .....	53
20. Grid visualizing the distortion in the 1st-order polynomial transformation .....	58
21. Average cell movement between the 1974 survey map and the rectified maps .....	60
22. Distribution of localized movement resulting from geo-rectification .....	61
23. Average cell movement between the 1974 survey map and the spline map .....	62
24. Cross section of Garmin 60CS recordings during five daily excursions .....	64
25. 2011 Limited field survey routes, middle Malpasó Valley, Zacatecas, MX .....	65
26. Example of ASL ambiguity between warped map and GPS recordings .....	66
27. Survey cells with validation data .....	67
28. Scatter plot of ASL positional difference .....	68
29. Distribution of 1974 estimation of site size for the middle Malpasó Valley .....	70
30. Adjust geo-rectified map produced from the 1974 survey map .....	81

## LIST OF TABLES

<b>Table</b>	<b>Page</b>
1. DEM Characteristics .....	33
2. Landsat 5 Characteristics .....	35
3. Peak Points Interpolation Program - Python Pseudocode.....	44
4. Input and Output Data of the Peak Points Interpolation Program .....	45
5. GCP Point Pair Creation Matrix .....	52
6. Geo-Rectification Polynomial Transformation Report.....	56
7. GPS to Geo-rectified ASL position .....	69
8. Consideration of site size in geo-rectification performance .....	71
9. Positional shift of 21 archaeological sites on the 1974 survey map (meters).....	74

## CHAPTER I

### INTRODUCTION

In 1974, Dr. Charles D. Trombold conducted an exhaustive field survey of the middle Malpaso Valley in Zacatecas, Mexico. The survey focused on confirming the existence of previously recorded archaeological sites and discovering undocumented sites. This research produced a hand drawn map, identifying the location of over 200 prehistoric archaeological sites (Figure 1). The map has undergone digitization and minor revisions over the years, but still remains in its original two-dimensional form. This research uses Geographical Information Science (GISc) methods to establish spatial information pertaining to archaeological sites within the middle Malpaso Valley. Analysis of residual and Root Mean Square Error of geo-rectification, the process of converting the map's cartographic coordinate system to a geographic coordinate system, produces both localized and overall geodetic accuracy assessments of the 1974 survey map. Ground control points acquired using Global Positioning System (GPS) provide a basis for establishing confidence in the geo-rectified map. This research is a technological continuation of previous work in the Malpaso Valley, and aims to produce a useful map for spatial analysis and data management in future research.

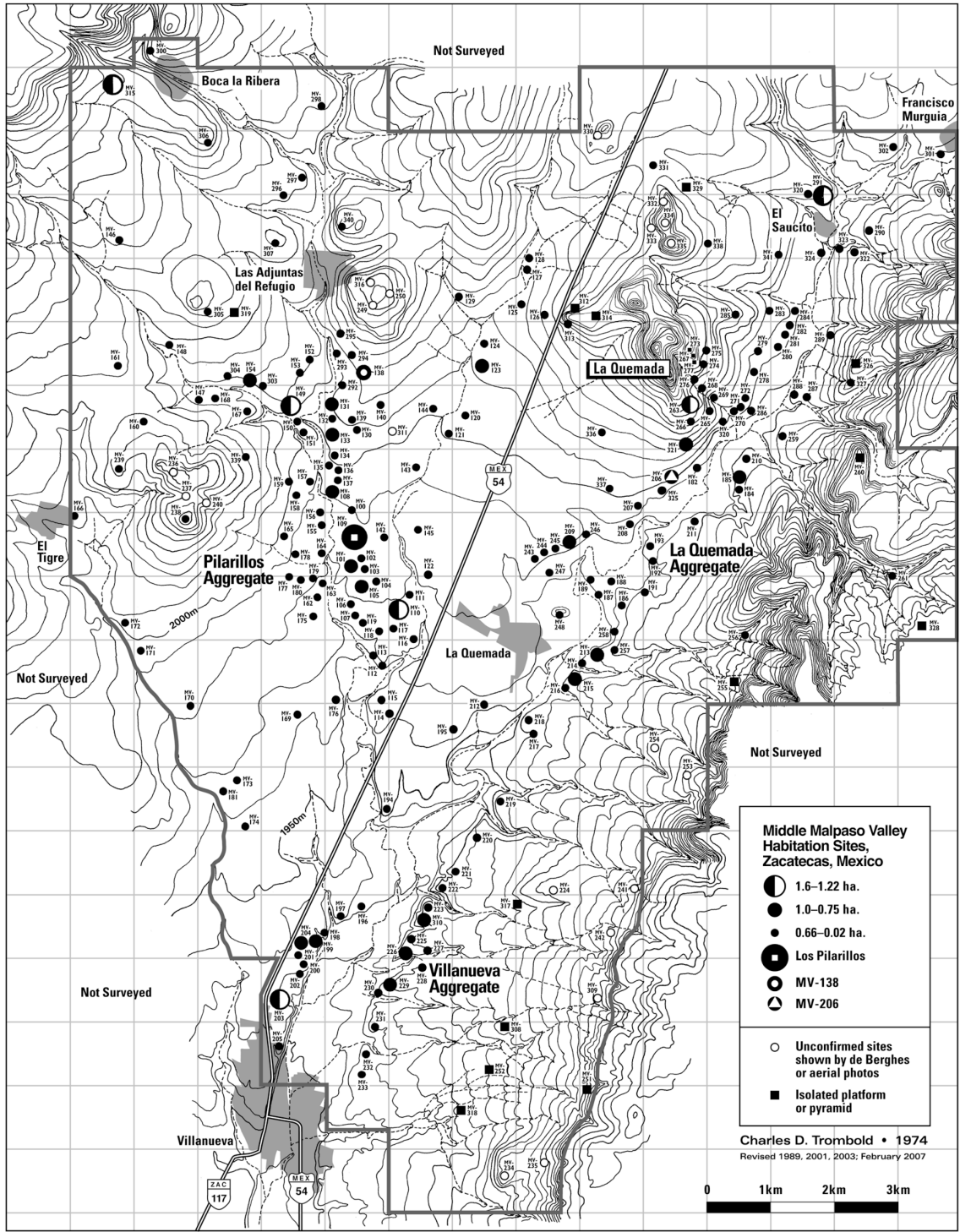


Figure 1. 1974 survey map

Archaeologists are continually exploring ways to improve their field methods. The field survey, the primary vehicle of exploring and gathering data for analysis, consists of a combination of procedures that include but are not limited to background research, analysis of remotely sensed imagery, and subsequent visual inspections (walking, driving, etc.) of the terrain to verify and discover evidence of human modification to the landscape. Maps created from a field survey are important records that reflect the spatial and temporal interaction of features on a landscape. Positional accuracy varies between maps, dependent on the intent to represent features as they relate to space (Blakemore and Harley 1980).

Before the advent of satellites and Global Positioning System (GPS), researchers created field survey maps using general descriptions, distance, and azimuth to demarcate landmarks, areas and objects of interest. Maps in general are by default abstract, in the sense that they are products of human interpretation of the landscape, and clarified as best as possible by science (Eckert 1908). Positional accuracy, a relative measure of closeness between a mapped location and its accepted true location, can vary greatly within a historic map and between multiple maps of the same area (Blakemore and Harley 1980). While most historic archaeological maps convey an overall sense of space, distribution, and serve as a guide to conduct follow up research at specific locations, their positional and geodetic accuracy may not support spatial analysis. Assessing a map's overall and localized positional accuracy is a key element of any research based on spatial analytical methodologies, including the one discussed in this thesis.

Positional accuracy has three dimensions: latitude, longitude, and elevation, and is measured independently for each dimension or as a summary value for all three. The coordinates of objects on the ground are often expressed in linear x and y values (e.g. meters) rather than in latitude and longitude, which are angles. If the three dimensions are not known, as is the case with the 1974 survey map, these attributes can be established through conducting a second field survey or using GISc. When developing an investigative strategy, time and money are highly correlated factors of a project (Black and Jolly 2003). This research explores GISc as an inexpensive solution to establishing dimensional data and improving a historic map's positional accuracy. Geo-rectification in GISc, a process commonly referred to as rubber-sheeting or warping, applies an image correction algorithm to stretch and pull the historic map onto a target, based on matching the location of features on the historic map to features on a target. The target, a source of higher accuracy with known dimensional attributes, includes but is not limited to aerial photography, remotely sensed satellite imagery, and maps of larger scale. Through geo-rectification, the map's components are assigned real-world dimensional attributes, which can be vetted through GPS and used to assess the map's positional accuracy.

## CHAPTER II

### PURPOSE

The objective of this work is to answer two research questions:

- 1) What is the positional accuracy of Trombold's 1974 archaeological survey map of the central portion of the Malpaso Valley, Zacatecas?
  
- 2) Is GISc's geo-rectification an acceptable substitute for conducting an additional field survey in order to establish dimensional attributes for the over 200 archaeological site locations (ASL) mapped in the 1974 survey?

To answer these questions, this study will investigate the process of geo-rectification of a hand-drawn ASL map of the middle Malpaso Valley, Zacatecas, Mexico. A rigorous historical investigation and visual analysis of the hand-drawn map will identify potential methods of control point selection. For each acceptable method, performance of the geo-rectification process in the form of the resulting residuals and Root Mean Square Error (RMSE) of the geometric transformation types: third-, second-, first-order polynomial, adjust, and spline will be analyzed for best-fit. A residual is a measure of distance between where the rectification process placed the map's control points to their corresponding real-world recorded locations. The residuals and the

calculation of RMSE, an index of error of all residuals, will result in an accuracy assessment of the geo-rectified process. Comparison between the dimensional attributes of the best-fit geo-rectified map and GPS collected control points will address if geo-rectification of the historic map results in an acceptable positional accuracy to use as a source of interpolating dimensional values for the ASLs.

This study will also produce local and regional values for the historic map's positional accuracy. These values typically vary across any given map, especially historic maps. A principle objective of this research is to identify outliers, including sections of the survey map that contain relatively high and low accuracy levels. Local information is an important input in addressing the second objective of this research. It serves as an input to the development of an optimal secondary survey strategy by presenting areas of low and high accuracy. If geo-rectification does not produce an overall acceptable positional accuracy, identifying sections of the map containing relatively high positional accuracy may preclude them from inclusion in a secondary survey. This will decrease overall time required to produce a new map of the middle Malpaso Valley with an overall acceptable level of positional accuracy.

In addition, this study will explore the potential for utilizing GISc software, programmatically, to automate data generation and the process of geo-rectification. Employing a high level programming language to automate processes will: 1) reduce the amount of time required to generate data and manage the process of executing multiple models of warping, 2) decrease the overall processing time by utilizing a computer's ability to run multiple processes concurrently, and 3) result in re-useable tools that will benefit the archaeological and geographic community.

Archaeological studies concerning the temporal period of the Mesoamerican northern frontier, within the Malpaso Valley and surrounding regions have recently begun to incorporate GISc in their data management and analysis (Elliott 2005; Ignacio and Quintero 2011). While important contributions to the archaeological record, the site attribute data produced, and subsequent analytical results, lack inter-study cohesiveness. In order to analyze relationships and conduct inclusive analysis of the Malpaso Valley's past cultures and their environment, a system, repository or vehicle is required to link everything together. Currently, no such system exists. Throughout a century of research, the Malpaso Valley has provided a wealth of information and data to the archaeological and historical record. Establishing a digital foundation in GIS will aid ongoing research and facilitate new endeavors within the area.

The first step in creating a digital foundation for the Malpaso Valley is to establish, with the highest accuracy as possible, the site locations. Producing a spatially accurate ASL map and developing a database of site attributes will create a common structure in which to tie together the hundreds, potentially thousands, of prehistoric and historic sites in and around the Malpaso Valley. An analysis of variance in the results of the rectification process on the 1974 survey map will determine the usefulness of the map in establishing the site's real-world location. Geo-referencing the prehistoric archaeological sites provides real world context to the site locations in the form of latitude and longitude values. Results of this research will directly influence the time and cost required to establish a digital foundation in GIS for the Malpaso Valley.

The results of this study will serve to compliment previous and ongoing research, initiated by Trombold's work. It will be especially beneficial to work in and around the

Malpaso Valley, which incorporates the historic map's site locations in any type of spatial analysis.

Establishing accurate geographic spatial reference for archaeological sites on this historic map is a precursor to a larger research endeavor: fostering archaeological and geographical research in the Sierra Madre Occidental. With accurate spatial information, future research can confidently associate natural and social landscape attribute data to the sites. The data created through this study is paramount in assessing the potential in the successful creation and implementation of a geographic location model of prehistoric sites within the middle Malpaso Valley. This model would be applicable to the numerous surrounding valleys within the region, which share similar physical and social context, to predict areas of high site location potentiality. Developing a predictability model will not only reduce the time required to conduct future archaeological surveys, it will provide a sound empirical base for creation and testing of regional cultural models.

## CHAPTER III

### SITE AND SITUATION

The central northwestern region of Mexico, once the Mesoamerican northern frontier, now supports large localized urban areas and mining operations. The Central Plateau of Mexico dominates the landscape, with the Sierra Madre Occidental mountain range to the west, and the Sierra Madre Oriental mountain range to the east. A network of long, narrow valleys connects the Central Plateau with the Pacific Ocean. This work focuses on the Malpaso Valley, located in a transitional zone between the Central Plateau and the Sierra Madre Occidental (Figure 2).

The valley is part of the headwaters to one of the largest hydrological basins in the Central Americas, the Santiago-Lerma river basin, which eventually drains into the Pacific Ocean (Figure 3). Characteristics of the basin include slow moving, meandering surface streams with the potential for seasonal flooding (Tamayo and West 1964). The region is considered a steppe climate based on the Köppen classification (Perry-Castañeda Library Map Collection 1975), with a current average temperature ranging from 12 to 20 degrees Celsius and an average precipitation of 500 to 800mm per year (INEGI 2011).



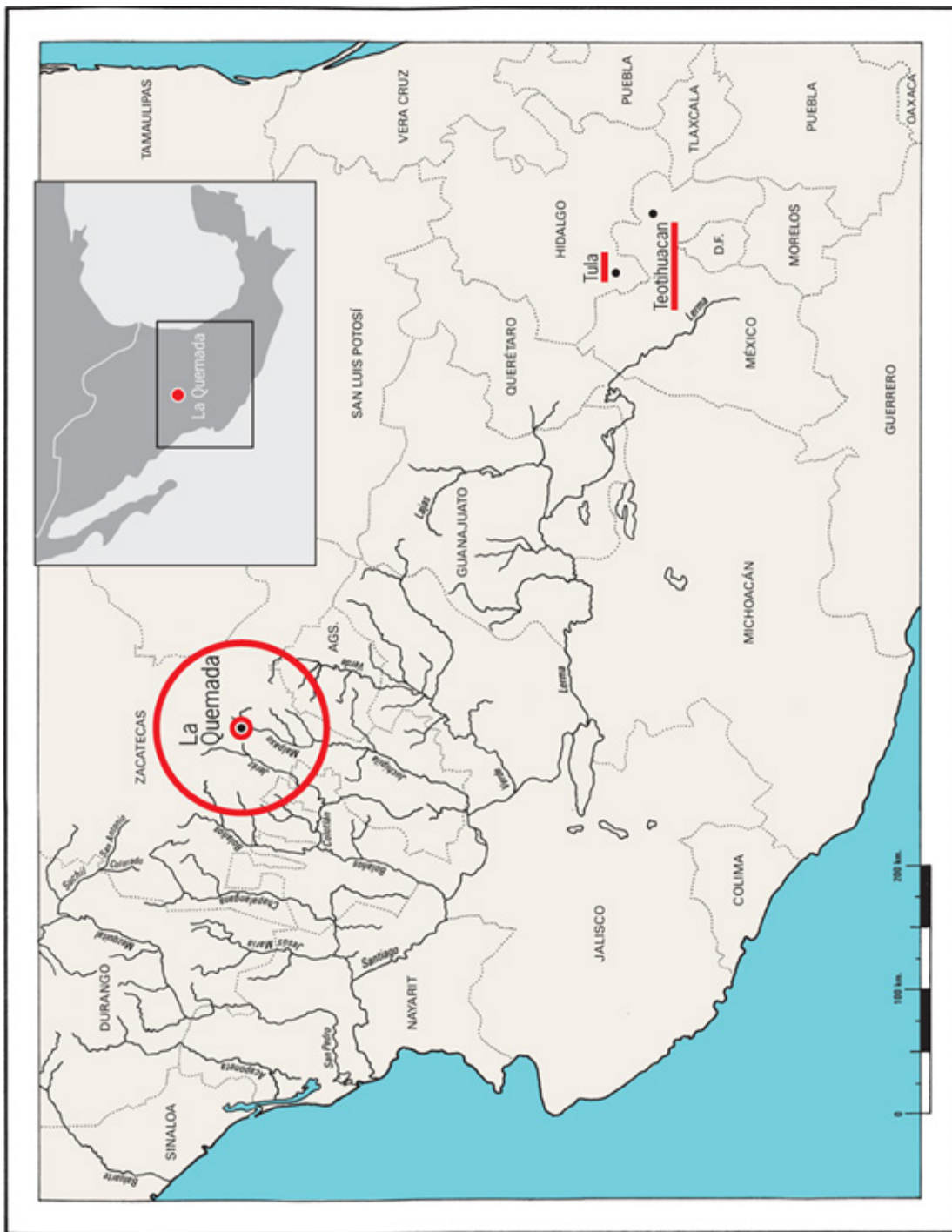


Figure 3. Santiago-Lerma drainage basin

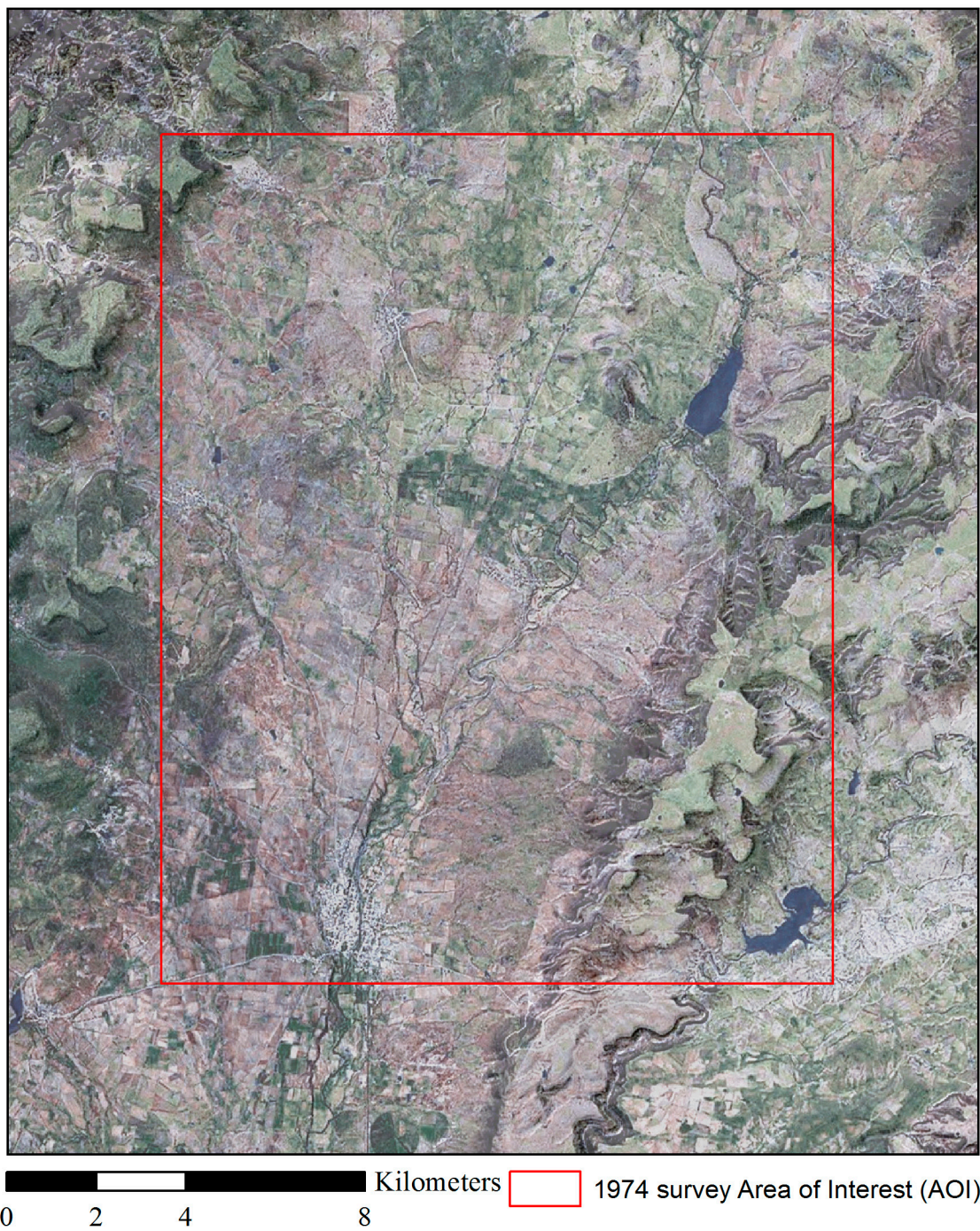


Figure 4. Middle Malpaso Valley, Zacatecas, Mexico

Beginning around AD 400, populations in the northern Mesoamerican frontier began to establish permanent settlements. In the middle Malpaso Valley (Figure 4), the major period of florescence occurred from ca. AD 650 to 850, after which the region

appeared to have been gradually but irreversibly abandoned (Kelley 1971; Trombold 2005b). Supported by a highly aggregated hinterland population, the site of La Quemada developed into a major civic/ceremonial center, and established a dominating presence on the landscape (Figure 5) (Trombold 2005b).



Figure 5. Ruins of La Quemada, south side

The Malpaso Valley influenced and helped shape the Mesoamerican northern frontier. Its location provides a route and potential link between the high Mexican Altiplano and the Pacific Ocean. La Quemada's socio-political complexity and influence has been analyzed (Elliott et al. 2010; Hers 1989; Ignacio and Quintero 2011; Jimenez Betts 1990; Nelson 1994; Trombold 1991; Trombold 1996; Wells 2000; Wells and Nelson 2002; Wiegand 1982), compared, and included in analysis between other regional and long-distance socio-economic centers (Figure 6) (Braun and Plog 1982; Kelley 1971;

McGuire et al. 1994; Nelson 1995; Neurath and Bahr 2005; Trombold 1976; Wilcox et al. 2008).



Figure 6. Northern Mesoamerican socio-economic centers (Ignacio and Quintero 2011)

When comparing La Quemada and the Malpaso Valley to other major Mesoamerican cultural areas, the amount of field research conducted in this valley is minimal. Physical evidence of trade with cultures surrounding the valley resides in the presence of a limited collection of artifacts and no written records of the indigenous culture survived or ever existed.

Between the 1600s and 1800s, European travelers visiting and working in this region began to develop the first written history of the area (Bancroft 1875; Batres 1903; Portillo and Weber 1935). Documents and journal entries describe a landscape full of grand edifices, abandoned and lying in ruin. In 1826, an English mining engineer,

Captain G. E. Lyons, published one of the first descriptions of La Quemada that included the importance of the surrounding settlements and road network. Following Lyon's work, in 1831, two German mining engineers, Carl deBerghes and Joseph Burkart, received a commission from the State Congress to produce detailed maps of La Quemada and its hinterland. These early works provided a foundation for which subsequent maps and analysis were based on, which in turn serve as the basis for modern maps (Trombold 1978).

Since then, only a handful of explorers and archaeologists have attempted to document and conduct field research in the hinterlands of La Quemada. Previous field research includes: ethnographic reports and travel journals by Aleš Hrdlička (1903) and Edward Seler (1908), Carlos Margain and Hugo Moedano's limited excavations in 1947, Pedro Armillas' survey in 1963, Charles D. Trombold's survey in 1974, surveys conducted during Ben Nelson's excavations in 1995 and 1997, Neill's work in 2003, survey data obtained during excavations by Charles D. Trombold in 1986, 2000 (Trombold 2005b), and more recent excavations in 2008.

Trombold's 1974 survey map and subsequent rectification, based on Carl deBerghes' map, represent the most complete and recent map documenting the middle Malpaso Valley as a system of La Quemada. The 1974 field survey lasted almost an entire year, resulting in a systematic 100% block survey, recording 235 sites. The resulting archaeological site map (Figure 1) has undergone minor revisions over the years, including a version published with prehistoric roadways (Trombold 1991), and the continual addition of recently discovered sites. This historic map provides the basis and framework of this research.

## CHAPTER IV

### LITERATURE REVIEW

Researchers, in a broad range of scientific research, utilize geo-rectification not only as a tool to create useable maps, but also as an integral component of data management. It is an important step in integrating maps and imagery with geospatial datasets (Rus et al. 2010). In environmental studies, geo-rectification aids in establishing accurate ground cover classification maps, detecting change in ground cover, and landscape planning and protection. For archaeologists, rectified remote sensed imagery provides a fundamental tool for current groundwork, analysis and management of data in GIS (Scardozzi 2009).

Positional accuracy is an important factor to consider during rectification. Acceptable values can range between projects, and vary depending on many factors. In 1998, the U.S. Department of the Interior, U.S. Geological Survey (USGS), National Mapping Division, developed the National Standard for Spatial Data Accuracy (NSSDA) for the Federal Geographic Data Committee. While the standard does not define threshold accuracy values, it does define spatial accuracy reporting requirements. According to the standard, Root Mean Square Error (RMSE) should be used to estimate positional accuracy, reported in ground distances at the 95% confidence level. Expanding on the standard, the NSSDA defines RMSE as the average set of squared differences between coordinate values between the source map and values from

an independent source of higher accuracy (FGDC 1998). This unnamed "independent source of higher accuracy" historically referred to airborne photography or to a larger scale map of known accuracy, which followed well-established standards during creation. Within the last decade, high-resolution satellite imagery acquired from sensors with a sub-meter optical scanning distance, has replaced airborne photography as the preferred source of accuracy for small to medium scale maps (Afify and Zhang 2008; Shaker et al. 2005).

Remotely sensed data, both on the horizontal and vertical plane, inherently requires preprocessing in the form of geometric and radiometric correction. As remote sensors orbit the Earth, the data they capture are not entirely nadir (directly below the sensor and perpendicular to the sensor surface). Applying geometric corrections to the recorded data correct for angular distortion. Additional radiometric corrections account for atmospheric interference and distortion (Fogel 1996). It is worthy to note that preprocessing of remotely sensed data corrects but does not eliminate accuracy error inherent in the remote sensors, causing a compounding effect on error when ortho- and geo-rectifying. Published accuracy values accompany remotely sensed data and are inputs to establishing confidence level in rectification. Analysis of current literature concerning preprocessing methods is beyond the scope of this paper.

In the world of computer science there exists a phrase, "garbage in, garbage out", which intends to highlight the fact that computers cannot output anything better than what the user inputs. The phrase can be modified to suit image manipulation to read "resolution in, resolution out". Computers, software and mathematical models cannot magically increase spatial resolution of image data. The accuracy of geo-rectification

directly correlates to and cannot exceed the accuracy of the reference data. McRoberts' (2010) investigated the effects of rectification and GPS errors on image classification, highlighting this fact. The study included a change detection analysis of 16 areas in northern Minnesota; each having an area around 15 km<sup>2</sup> with a mixed coverage of forest, agriculture and water. The researcher suggests that when the combined error of rectification and GPS reaches a value equal to that of the spatial resolution, more than half of the subplots (area defined with a 7.32-meter radius) receive incorrect values, introducing classification errors. This research clearly indicates the need for "the investigation of methods for correcting or compensating for [rectification and GPS errors]".

While data collection introduces potential sources of error, it is not the only instance where errors can occur during rectification. Smith and Atkinson's (2001) study "has shown that a large amount of error can be introduced simply by using different techniques to gather GCPs when rectifying images". The researchers used affine coordinate transformation to rectify two images acquired from remote satellite sensors. One set of GCPs were generated from digitized 1:24,000 scale United States Geological Survey (USGS) topographic maps and three sets were derived from various permutations of data collected using a Trimble GeoExplorer<sup>TM</sup> handheld GPS receiver. An initial group consisting of 26 GCPs were selected based on prominent, man-made surface features that were easily identifiable on both images and the topographic map. Based on RMSE, GCPs from GPS resulted in the best rectification accuracy. Additionally, they suggest that the most important criterion to GCP selection for rectification is to "match the resolution of the images to the accuracy of the GCP source".

Gaining an understanding the historical map in question is paramount in selecting good GCPs. Benavides and Koster (2006) address the question of historical map's usability: are historical maps reliable enough to use in spatial analysis? The researchers propose a model to assess various forms of historical maps. They identify a primary task: gain knowledge of the historical context and conventions used in production of the map. As a case study, the researchers compare historical cadastral maps of the Dutch town Zwolle to modern data. Through historical research, they developed an understanding the map design and features, which aided in selecting and refining a method of establishing GCPs. They also note that although a historic map may have high precision, that does not necessarily correlate to improving the ability to identify reliable GCPs. In conclusion, their case study supports their hypothesis that "correct interpretation of features depicted on historical maps...will reduce the number of errors [made] in processing and therefore lead to a more reliable use of digital maps". The ability to select reliable GCPs is a crucial factor in achieving an accurate assessment of a historical map's usability.

Once a historical map has undergone a process of vetting, it is important to understand the spatial accuracy of the target data. Remote sensed imagery, serving as a target data set, undergoes correction methods known as ortho-rectification and radiometric correction. As with geo-rectification, ortho-rectification employs various mathematical models to transform data between image space and object space by removing terrain distortion (Afify and Zhang 2008; Fogel 1996; Shaker et al. 2005). While not the type of rectification utilized in this study, modern archaeological research incorporates, and relies on ortho-rectified high-resolution imagery. It is imperative to

understand the geometric correction methods used to achieve horizontal and vertical accuracy of remotely sensed data. This method ultimately produces a spatial context (reference data) in which hand drawn maps are stretched and warped onto through georectification.

During the early development of rectification, Fogel (1996) addressed the shortcomings of the then preferred mathematical methods of image warping/rectification: bivariate mapping polynomials and piecewise linear finite elements. These shortcomings were well documented and are in essence, the methods currently associated with georectification. Fogel goes on to introduce and analyze newer methods based on radial basis functions: Hardy's multiquadratics (MQ) and thin plate splines (TPS). The study area consisted of a facility formerly involved in nuclear component production, occupying eleven square miles, including a buffer zone, with an elevation change of 600 feet. Fogel established 98 ground control points (GCP) and 24 check points derived from imagery. Adequacy of the sample and overall model fit was evaluated using cross validation. This author concluded that image rectification using MQ and TPS outperformed bivariate mapping polynomials in both RMSE and visual inspection. The results of this study highlight a period when ortho-rectification began advancing, along with technology, in a direction towards more complex mathematical methods in establishing higher accuracy.

Fogel also noted the limitation of accuracy in extracting GCPs from imagery. The proliferation of GPS and processing techniques alleviated this inaccuracy by the early 2000s, providing GCPs within an area of interest, with an accuracy of 2.5 meters. Research conducted by Satirapod et al. (2003) investigated the use of dual-frequency GPS receivers in combination with post-mission information and advanced data

processing techniques. Their results demonstrated that a horizontal accuracy better than 2.5 meters was obtainable in establishing GCPs.

With the advent of sub-meter remote sensors and processed GPS data providing GCP accuracy less than 5 cm, innovative researchers continued to push the boundaries and advance ortho-rectification methods. Polynomial methods experienced resurgence in 2D models. Ward (2005) examined an approximation algorithm using 2D Chebyshev polynomials. Shaker et al. (2005) conducted an ortho-rectification study incorporating four 2D polynomial models and one projective model to determine effect of land topography, best 2D model, and optimum number of GCPs. To discover any effects of terrain variation on the model's accuracy, the authors chose two distinct topographic datasets of equal area ( $\sim 11\text{km}^2$ ): the city of Zagazig in Egypt (a relatively flat area) and a hilly area of Hong Kong. While examining GCP selection methods, Shaker et al. acknowledges the importance of GCPs derived from topographic maps and digitized tablets, but also state that GCPs derived from dual GPS receivers resulted in a spatial accuracy closer to that of the satellite imagery (sub-meter). A lack of sufficient GCPs prevented the researchers from conducting higher magnitude polynomial models on the Zagazig dataset. However, first and second order polynomial models sufficiently resulted in sub-meter accuracy ( $\text{RMSE} < 1$ ) using a modest number (6) of GCPs. Pre-analysis of the Hong Kong dataset and GCPs exposed an expected absolute planimetric error ranging from 1 to 111 meters directly correlating with elevation. Due to this, Shaker et al. ran the five models using the original Hong Kong GCPs, and again with GCPs that underwent a transformation process involving an elevation compensation plane. The original GCPs produced a RMSE of up to 38+ meters, while their projected counterparts resulted in

RMSE values  $< 1$  in both X and Y directions. The authors concluded that the accuracy of 2D ortho-rectification of high-resolution satellite imagery is affected heavily by elevation, and their findings suggested that GCP quality and evenness of distribution is more important than quantity.

Researchers have continued to improve the mathematical models used in ortho-rectification of satellite imagery. In the mid-2000s, rigorous and non-rigorous 3D models superseded 2D models (Boccardo et al. 2004). As privatization of remotely sensed data increased, the availability of information required to perform the transformation between image space and 3D object space decreased. Companies that distributed imagery were not always forthcoming with the rational function coefficients (RFC) required to conduct 3D rigorous modeling. The introduction of 3D Rational Function Model (RFM) attempted to circumvent this lack of information. RFM is explained by both Boccardo et al. (2004) and Afify and Zhang (2008) as a non-parametric model (general/empirical) independent of the platform, sensor, acquisition method, and projection system. The 3D RFM can be run with either vendor-supplied or user-derived RFCs.

Acknowledging previous research in establishing accuracy with 3D rigorous modeling and 3D RFM with vendor-supplied RFCs, Afify and Zhang (2008) investigated the accuracy of 3D RFM incorporating user derived RFCs from GCPs. Their research aimed to assess geometric accuracy derived RFMs, compare 3D RFM performance of multiple polynomial transformations using user-derived RFCs, and determine optimal number of GCPs for each 3D RFM. The study area included a town in New Brunswick, Canada, chosen for its extensive road network, which aided in the establishment of GCPs. Total elevation change of the study area is about 250 meters. The authors derived

coordinates of GCPs and checkpoints from a combination of vector maps and a digital terrain model. After running the models, Afify and Zhang (2008) concluded, "the higher the order of the used RFM, the higher the geometric accuracy obtained." Resulting RMSE of 1.45 and 2.16 meters, using 39 GCPs for third order 3D RFM demonstrated that the use of user-defined RFCs in a 3D RFM provides competitive accuracies when compared to 3D rigorous models and 3D RFMs with vendor-supplied RFCs. While their method of establishing GCPs resulted in a respectable accuracy (RMSE) of 2.5 meters, a set of GCPs derived from GPS, as shown by Shaker et al. (2005), may have produced lower RMSE values for all models run in this study.

Recent research by Gil et al. (2011) validates current 3D methods through a case study incorporating 3D rigorous models and 3D RFM with vendor supplied RFCs. Their study includes an analysis of accuracy and number of required GCPs in ortho-rectification of high-resolution satellite imagery over an area of mountainous relief. The conclusions are consistent with other current studies.

Focusing on rectification and its role in archaeology, archaeologists understand that the landscape itself patterns where cultures choose to interact with their landscape (Kvamme 2006). Prehistoric environments differed greatly spatially and temporally. Due to this diversity, establishing ASL at a regional level, within a focused temporal period results in the highest level of spatial accuracy. While it is impossible to recreate the exact past landscape, understanding the current landscape provides a real-world context for archaeological subject matter (Black and Jolly 2003). From observing relationships between archaeological sites and landscape, we can learn something about how they interacted with the environment (Kvamme 2006). Scardozzi (2009) presents an excellent

paper concerning the establishment of this relationship through the contribution of ortho-rectified high-resolution satellite imagery. Due to the remote nature of his research area of interest in Turkey and Iraq, large-scale maps and aerial photography were not available. Using differential GPS, he established GCPs, and in conjunction with a digital elevation model (DEM), ortho-rectified two sets of high-resolution satellite data. This resulted in the production of accurate base maps and cartographies, useful tools employed while conducting ground surveys and managing research data in GIS. Using the ortho-rectified data as a source of higher accuracy (FGDC 1998), Scardozzi was able to subsequently apply the process of geo-rectification to old archaeological maps, plans of excavated structures, archaeological data and paleo-environmental elements, bringing real-world context to the archaeological record.

Other recent articles (Bruna et al. 2010; Timar and Mugnier 2010; Witschas 2003) reiterate the importance of historic cartographic documents, as they represent a valuable source of information in the reconstruction of the past environment. Historical maps typically appear in one of two forms: cadastral and navigation/orientation. Cadastral maps represent land holdings and urban design, while navigation maps encompass general landscape features, used primarily for military and exploratory orientation (Podobnikar 2010). Current research and literature suggests varied approaches to establishing GCPs when geo-rectifying historic maps. Identifying features and places on historic maps suitable to establish GCPs for geo-rectification is subjective and differs for each application. At time of creation, historic maps were not only influenced by the artistic style of the mapmaker, their production methods were bound by the concurrent development of techniques, mathematical knowledge and availability of resources

(Podobnikar 2010). Therefore, each site, situation, and purpose is unique, defining its own acceptable accuracy of geospatial positioning.

In light of the meticulous nature in GCP selection, the process of selecting control points on a historic map does not appear to qualify as a candidate for computerized automation. Surprisingly, some amount of success is achievable through the implementation of automation, specifically pertaining to maps containing gridlines or other means of entire-map scale demarcation. Rus et al. (2010) established GCPs on historic Romanian maps using computer software to identify points and their spatial correlation based on a grid, built from the map's regulated graticule grid. This proves to be extremely helpful when geo-rectifying a large quantity of maps similar in cartographic design. Just as automation can improve the performance of applying one process to many maps, it can also improve the inverse, where many processes are applied to one map, which is the case in this work.

## CHAPTER V

### METHODOLOGY

#### **Data Acquisition**

##### 1974 Survey Map

Trombold provided a digital copy of an updated 1974 ASL map of the middle Malpas Valley and attribute data pertaining to the sites. The map covers a 285 km<sup>2</sup> area, containing hand drawn city boundaries, major modern road network, watershed drainage system, terrain relief and elevation (in the form of topology lines), and prehistoric archaeological site locations. The map is a Tagged Image File Format (TIFF) raster data set containing 7303x9380 pixels (cells) at a resolution of 600 pixels per inch, which puts the map at a scale of almost 1:50,000 (Figure 1).

Understanding the process of design and cartographic methods associated with the creation of the historic map is critical in developing a GCP selection strategy (Benavides and Koster 2006). Neither metadata nor published information concerning the methods used to create the map is available. However, personal communications with the original cartographers is currently possible. According to Dr. Trombold (personal communication May 26, 2012), many parties contributed to the map creation process, from preliminary research, to final digital production.

An investigation of the methods used in the field to generate the map sets the premise for its creation and develops the map's history. Before the survey began, black

and white aerial photography and a topographic map were acquired from Comisión de Estudios del Territorio Nacional (CETENAL), now Instituto Nacional de Estadística y Geografía (INEGI), of Mexico. The images were part of CETENAL's 1969 campaign to create a national set of topographic maps. Three fixed cameras mounted on an airplane flying east-west routes recorded two sets of images. One camera was mounted nadir and a pair was mounted oblique to create stereo pairs. CETENAL acquired the images during the dry season, reducing the amount of vegetation present. The lack of ground cover, coupled with high-resolution photography, captured an obstructed view of the terrain in which individual trees, automobiles and distinct structures are visible. The first set of images, available as large prints (50cm x 50cm) at a scale of 1:12,500 covered 6.25 square kilometers each. The other set of aerial photographs were stereo pairs at a scale of 1:25,000. Stereo pair photographs, when placed side by side and viewed through a stereoscope, create a 3D optical illusion. The Mexican Government produced topographic maps at a scale of 1:50,000 from these images, which are still in use today. The maps contained contour lines at an interval of 10 meters. For the field survey, Trombold acquired topographic map number 'Villanueva F-13-B-77'. No information concerning ortho-rectification and the process of interpolating of the aerial photographs to produce the topographic maps became known during the course of this research.

During the field survey, Trombold carried the large 1:12,500 scale images, topographic map, a copy of the deBerghes map, and an additional map based on the deBerghes map published by Guillemin Tarayre in 1869. Traversing the valley on foot without a compass and relying on common sense aided by the images and both maps, he systematically inspected the landscape for evidence of prehistoric human activity. Upon

confirmation or discovery of an archaeological site, he established positional accuracy using the topographic map and photo images. He then penciled the site outline directly onto the aerial photos and topographic map. Although the stereo pair set was rarely used in the field, due to the scale and delicate nature of aligning the two photographs under the special viewer, stereo pair imagery did provide ancillary data before and after a day's survey.

After completion of the field survey, Dr. Trombold returned to Southern Illinois University (SIU). There, the Geography Department mechanically created a master ASL map of the middle Malpaso Valley. First, a new map was hand-drawn using the CETENAL topographic map as a guide. The contour lines, hydrological features, and roads were reproduced on the new map. It is unknown if the contour lines were traced using an enlarger, or drawn freehand. Next, the site locations and terraces were transcribed from the images to the map, drawn in ink at their proper location. A professional typesetter provided additional type setting which was cut down to size with a razor blade and affixed to the map with melted bees wax. The finished product was then carefully delivered to a printer to be photostated, a process in which a photograph of the map is taken, and printed directly onto a Mylar master. Later, Michael Simpson digitized the 1974 ASL map, adding an arbitrary graticule in 1-kilometer intervals and performing revisions in 1989, 2001, 2003, and 2007 in St. Louis, Missouri.

Throughout this entire process, situations may have occurred which created environments that may have allowed errors to enter into the process of establishing site locations on the map. In the field, under duress and presented with a homogenous terrain, a surveyor may become disoriented and mark a site in an incorrect location. The

topographic map, being an interpolated surface, may not accurately reflect the terrain's slope and aspect, causing a site to be slightly mismarked. Slope, the change in elevation over a distance, may appear congruent with the topographic map at an incorrect location. Aspect, the direction in which the slope is facing, may confuse the surveyor in mountainous areas where the aspect may change rapidly. Errors may have occurred during the manual process of transcribing the contour lines and recreating the penciled site location markings when creating the master ASL map. There exists a potential for the errors to create a compounding effect in the site's positional inaccuracy. However, the scale of the imagery used in the survey and inherent size of the archaeological sites may negate any positional errors. If, according to Dr. Trombold, distinct highway lanes and automobiles were clearly visible when viewing the imagery, archaeological sites with any surface anomalies would also be visible, and easily matched to the recordings made in the field.

Along with the ASL map, Trombold produced a table of attribute data associated with the archaeological sites, which includes but is not limited to: function, classification, estimated size, surface artifacts, biotic community, drainage classification and Euclidian distances to environmental features. The attribute data may be beneficial in future studies focusing on conducting updated spatial analysis such as site clustering, cost-weighted routing, and social hierarchy network analysis.

#### Digital Elevation Models

The other major component to geo-rectification is data sources of higher accuracy (targets). Due to the study area's remote nature, there is a lack of free high-resolution digital imagery. It is possible to acquire remotely sensed imagery of the valley through

private businesses, but the cost is well outside of this work's budget. Choosing to use a DEM in combination with imagery as the target source will ensure continuity between ASL positional attributes and elevation values after geo-rectification.

Two DEMs published by Mexico's Instituto Nacional de Estadística y Geografía (INEGI) are available free of charge. The two DEM's (version 1 and 2) cell resolution is 1 arc-second (30 meters) with an unknown vertical accuracy and horizontal resolution. They are distributed in Band Interleaved by Line (BIL) format and use the International Terrestrial Reference Frame 1992 (ITRF92) as its datum to establish spatial information. I hypothesize that both DEMs are interpolated from the topographic maps, which were interpolated from the previously described aerial photography taken in 1969. According to INEGI's website (2012), version 2 is based on continuous contour maps at 1:50,000 scale. While I could not locate any metadata, there are striking similarities between CETENAL's topographic maps, which are the same scale as the DEM sources. Throughout the DEMs, slope and aspect follow a smoothed, generalized terrain topography, matched by the topographic map. There are horizontal and vertical artifacts present throughout version 1, indicating that it may have been generated from digitizing a paper map. Figure 7 highlights a vertical artifact located in the top center, appearing as a linear section of pixels with colors that are in sharp contrast to its surrounding. An artifact is an unnaturally occurring section of a DEM that contains false elevation values. The artifacts may represent a number of issues, including processing errors in digitization, fold creases, and markings on the source map. The artifacts are localized errors, which may hinder establishing GCPs, but are not an indication of overall inaccuracy.

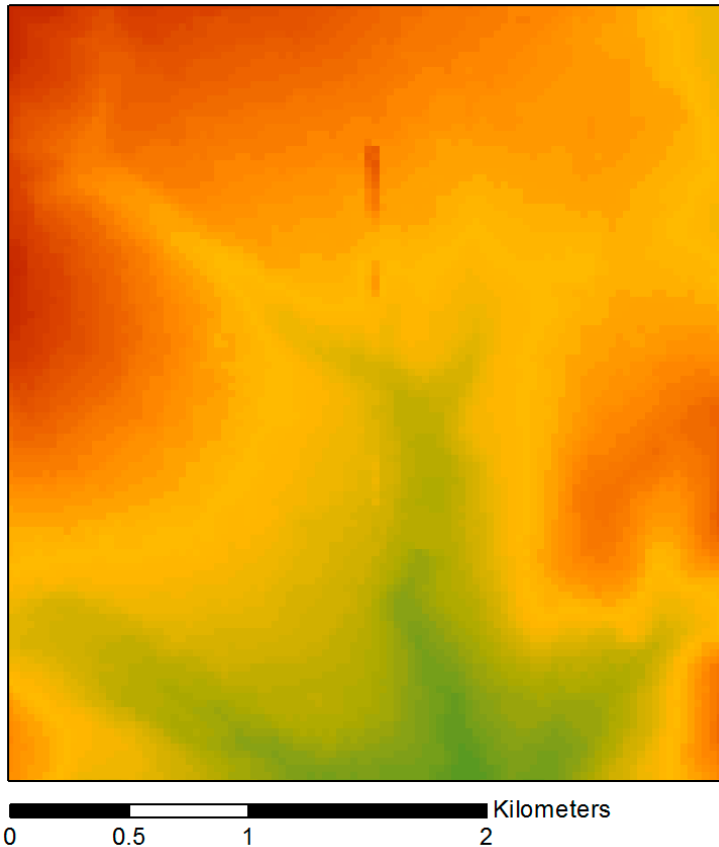


Figure 7. Example of a vertical artifact in version 1

According to INEGI, version 2, based on an interpolation model called ANUDEM, “relies significantly on other types of information [besides contour lines] such as... continuous river networks and bodies of water.” While this interpolation model contains many desired features, it introduces the need for additional processing to adjust the values along hydrological features (Hutchinson et al 2011). Performing the necessary corrections is outside of the scope and ability of this work. In original form, the data values for peaks and fields retain their familiar smooth transitioning slope, but the slope is grossly inaccurate near river systems and bodies of water, which appear as sinks (Figure 8). A sink is a section of a DEM containing false elevation values, which may be useful in specific applications.

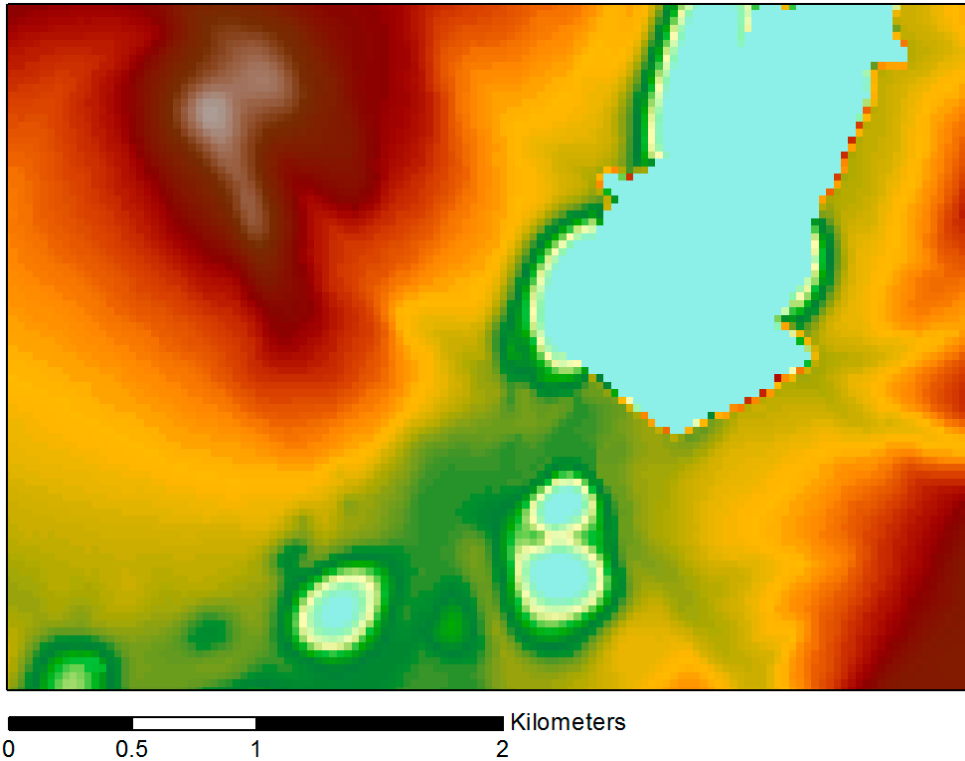


Figure 8. Example of a lake as a sink in version 2

As in version 1, these inaccuracies present minor barriers in implementing a methodology of establishing GCPs. Considering the probability that both DEM versions and the 1974 ASL map are interpolated from the same topographic maps, based on the same photographic imagery used during the field survey, supports their candidacy for inclusion as targets.

Additionally, a DEM is available from National Aeronautics and Space Administration (NASA) and the Ministry of Economy, Trade and Industry (METI) of Japan. In 2011, they released version 2 of a Global Digital Elevation Model (GDEMv2) from the Advanced Spaceborne Thermal Emission and Reflection Radiometer (ASTER). The GDEMv2's cell resolution is 1 arc-second (about 30 meters) with an average vertical accuracy of -0.20 meters and a horizontal accuracy of 71 to 82 meters (Table 1). It is

distributed as a Georeferenced Tagged Image File Format (GeoTIFF) file and uses the 1984 World Geodetic System (WGS84) / 1996 Earth Gravitational Model geoid to establish spatial information.

Table 1. DEM Characteristics			
Source	ASTER		INEGI
Version	ASTER GDEMv2	DEMv1	DEMv2
Pixel size (at Equator)	1 arc-second (~30 m)		
Vertical accuracy at 95%	17 meters	Unknown	
Horizontal accuracy	71 to 82 m	Unknown	

Visual analysis of the GDEMv2 presents a much higher level of precision over the two from INEGI. Precision indicators include the major roadway traversing the valley, clearly visible in the GDEMv2, and definition of subtle terrain nuances (Figure 9).

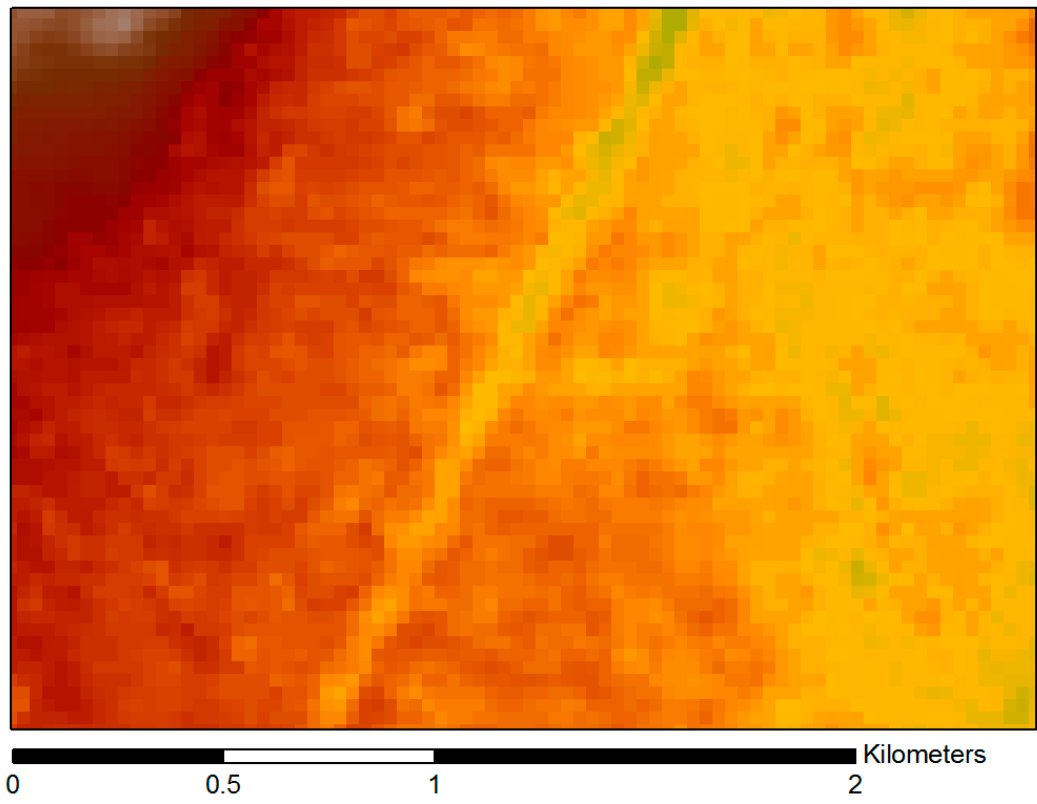


Figure 9. GDEMv2 example showing roadway and irregularities

However, it is not without issues pertaining to qualifying as a candidate as a target. Meyer's summary report cites that above ground features, including tree canopy and built structures clearly influenced the DEM by introducing a positive bias. This bias, combined with inaccuracies in ortho-rectifying high-resolution imagery (Shaker et al. 2005), result in a DEM with jagged and irregular slope and aspect.

Horizontal resolution of a DEM is important, as it impacts the interpolation algorithm responsible for generating contour lines. These lines are a critical component in the process of identifying matching peaks and gullies for GCP selection. Noting that the horizontal resolution is lower than the pixel size, this will result in less crisp ridges and gullies when viewing the dataset as a raster image. The slightly lower ridge elevations and slightly higher gulley elevations still produce a similar slope value compared to a dataset with higher horizontal accuracy (Meyer 2011).

#### Other Imagery

NASA's Landsat 5 satellite with a Thematic Mapper(TM) sensor furnished additional remotely sensed imagery. This multi-spectral dataset contains seven bands of land cover at a 30-meter spatial resolution and contains data for the visible and infrared wavelengths. Landsat 5's seven bands are superior to previous Landsat imagery, which were limited to the visible spectrum. Due to the launch of Landsat 5 in the early 1980s, spatial and temporal coverage gaps in image acquisition, cloud cover, and poor image quality, the temporally closest image available to the 1974 field survey is from April 1986. While current satellites do provide higher spectral and spatial resolution, the Landsat 5 imagery is sufficient for identifying terrain features such as river channels and flood plains, and it is accessible at no cost. The geometric accuracy for Landsat TM

imagery is an RMSE(net) of +/- 50 meters, specified by NASA's contract NAS13-98046 with Earth Satellite Corporation (Table 2) (Lockheed Martin Space Operations 2004).

Table 2. Landsat 5 Characteristics	
Pixel size (at Equator)	1 arc-second (~30 m)
Absolute vertical accuracy (average)	Unknown
Vertical accuracy at 95%	Unknown
Horizontal resolution	+/- 50 m

### **GCP Selection Method**

#### 1974 Survey Map Assessment

The quality and quantity of features on a historic survey map define and limit potential GCP selection methodologies (Blakemore and Harley 1980). Visual analysis of the 1974 survey map results in four feature classifications: natural, modern, prehistoric, and graticule. This low value is expected and normal considering the narrow goal of the map: to convey the terrain and relative locations of prehistoric archaeological sites. One would not expect complex urban street networks and inclusive land-use classification to be present on a historic ASL map of a remote valley. Features, which are included but not directly related to the goal, may be abstract and for reference use only. This is the case with the map's urban areas and major highway; they are abstractly demarcated and for reference only (personal communication Trombold 2011). A map's graticule is an excellent source of establishing GCPs, but the graticule on this map is for scale purposes only. Trombold dictated that it is an arbitrarily placed grid and the intersections have no dimensional attributes. A systematic inspection of the interaction between the graticule's intersections and the contour lines and streams hoped to yield an intersection, which could be identifiable on a topographic source of higher accuracy. If confidence in the

dimensional attributes of just one graticule intersection is established, then dimensional attributes can be calculated for the entire graticule. Unfortunately, this scenario did not occur. The only acceptable features for establishing GCPs are the map's contour lines and stream network.

### Valleys

In visualization software, assigning Landsat 5 infrared bands to any of the three-color channels (RGB) creates a false color image. By associating band seven with the red channel, band four with the green channel, and band two with the blue channel, the resulting false color image highlights sources of water and defines present and past river channels. Besides irrigated farmland, these are the only locations with dense vegetation during the dry season. The historic map's river network and Landsat 5 river channels are common map features that serve as a source in selecting GCPs in the area's valleys (Figure 10). You can clearly see on the Landsat 5 imagery where the river channel has deviated from its recorded position in 1974. The current channel is in blue, while past channels are in green, owing to the presence of vegetation that continues to exist along the old channels. In addition, GISc software has the ability to create a stream network from a DEM (ESRI 2012). A complex model creates a visual representation of the terrain's drainage paths created by low points and flow direction of a terrain (Figure 9). This network proves another source of higher accuracy for establishing GCPs in the valleys.

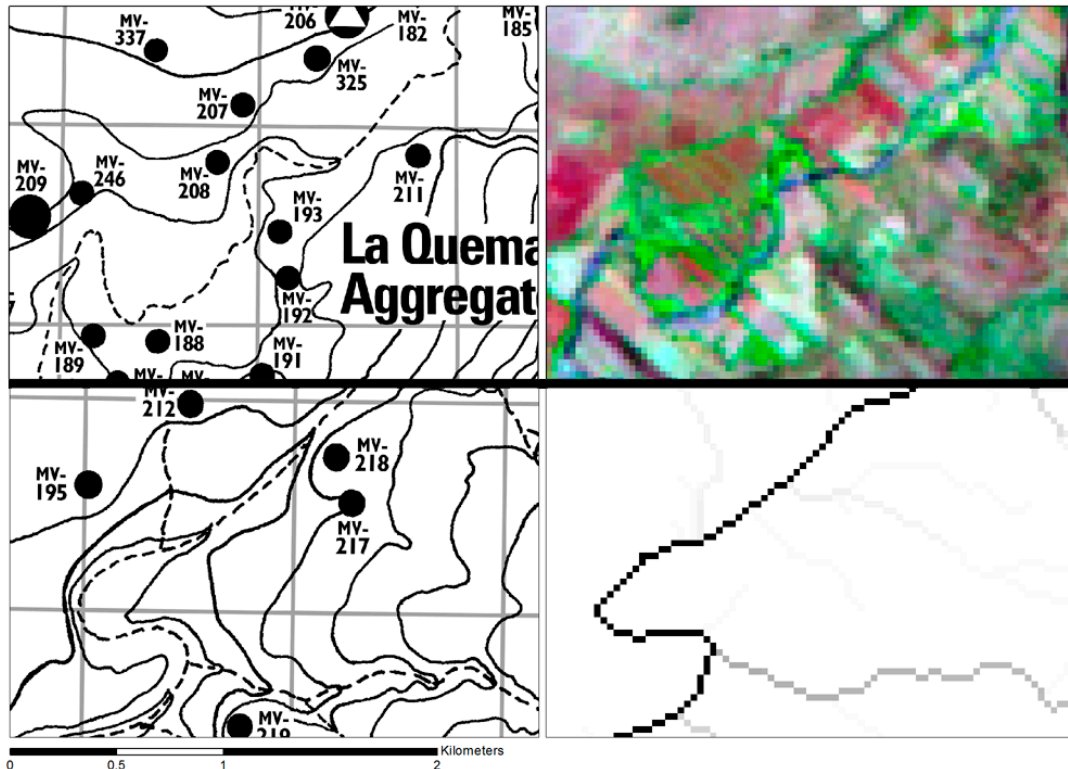


Figure 10. 1974 survey map river channels compared to Landsat 5 and river network

### Peaks

In this study, the process of establishing GCPs between the peaks on the historic map and the peaks on a target DEM is complex. Due to the presence of three potential targets, an issue arises regarding which one, or combination best represents the real-world peak locations. Arguments for and against each DEM appeared in the Data Acquisition: Digital Elevation Models section of this chapter. The lack of a nearby geodetic datum, a network of points on the Earth with known dimensional attributes, hinders the ability to establish local positional accuracy of the DEM data in the study area. Using GPS to record dimensional attributes for peaks within the middle Malpaso Valley is an acceptable method for establishing geodetic points, but acquiring those would defeat the purpose of this work.

GISc software converted and displayed all three DEMs in a common projected coordinate system, Universal Transverse Mercator (UTM) Zone 13Q using the WGS84 datum, to visualize the differences between the surfaces. UTM was chosen due to its ability to produce low distortion in a large north-south extent, matching this work's area of interest. Low distortion is due to the localization of the UTM system, which divides the surface of the Earth into 60 individually projected zones, each covering 6 degrees of longitude in width (USGS 2012). UTM is accurate to less than 1 mm in each zone (Karney 2011). UTM will be used exclusively throughout this work to maintain uniformity

Results were clear variations in cell values between all three, highlighting the differences in data acquisition and interpolation methods used to generate the DEMs. Analyzing the peaks' variance in dimensional attributes will result in quantitative values that may uncover systematic differences between DEMs. If the differences are random, calculating mean peak locations may provide an acceptable choice for establishing GCPs. If the mean positional difference is within the common pixel size of 30 meters, then using mean peak location represents a relative positional accuracy. This analysis will also establish a hypothesis addressing this work's main research questions.

The first step in analyzing peak locations is to establish the peaks' dimensional attributes. The most obvious response is to use the cell values of the DEMs to identify the "highest" cell for each peak. Cells with the highest value clearly represent a local high point in the data set. While this does result in the absolute highest point, it does not necessarily represent the naturally occurring peak of a hilltop. A false peak location may be generated by non-surface objects and natural and unnatural modifications over time.

For example, if there is a building located off-center on a hilltop creating a positive elevation bias, as is with the GDEMv2, a false peak location is generated. Without a priori knowledge of that hilltop, we then erroneously accept the highest cell value as the hilltop peak. Likewise, if a large pit is present at the location where the peak would naturally occur, this anomaly will cause the cells representing the dumped fill to contain the highest elevation value. These situations are often the case in archaeologically rich areas due to the presence of prehistoric and historic buildings location on hilltops, looters, and mining activities. Human activity is not the only cause of potential false peak locations. Breaks of trees on a hilltop have the potential to influence recorded elevation data on a seasonal basis. When comparing historic DEMs to present-day DEMs, the landscape may have changed over time. Uneven rates of erosion give obtuse hilltop topology, and can create multiple absolute peak locations.

For this work, using interpolated hilltop centroids, instead of maximum pixel values in a GCP selection methodology will result in an acceptable positional accuracy concerning this research when rectifying the historic survey map. Interpolating hilltop centroids in a diverse landscape is challenging. I employed a methodology combining the manual selection of optimal contour lines and an automated process to create interpolated peak points generates a data set from an unlimited number of DEMs. Using ESRI's ArcGIS Desktop (ArcMap, ArcCatalog), the DEMs were clipped to an area of interest 25% larger than the study area. This produced a smaller, more manageable elevation data set while ensuring contour lines along the boundary of the study area will be interpolated accurately. ESRI's Spatial Analysis module contains a tool that generates contour lines from a DEM by interpolating the surface and creating best-fit lines along the surface at

specified intervals. Contour lines at 5-meter intervals were generated from the DEMs, producing data sets of lines representing contours of the landscape with an associated identification value (ID) and elevation value. The three topographic data sets were loaded into ArcMap and displayed simultaneously, highlighting the differences in DEM cell values (Figure 11).

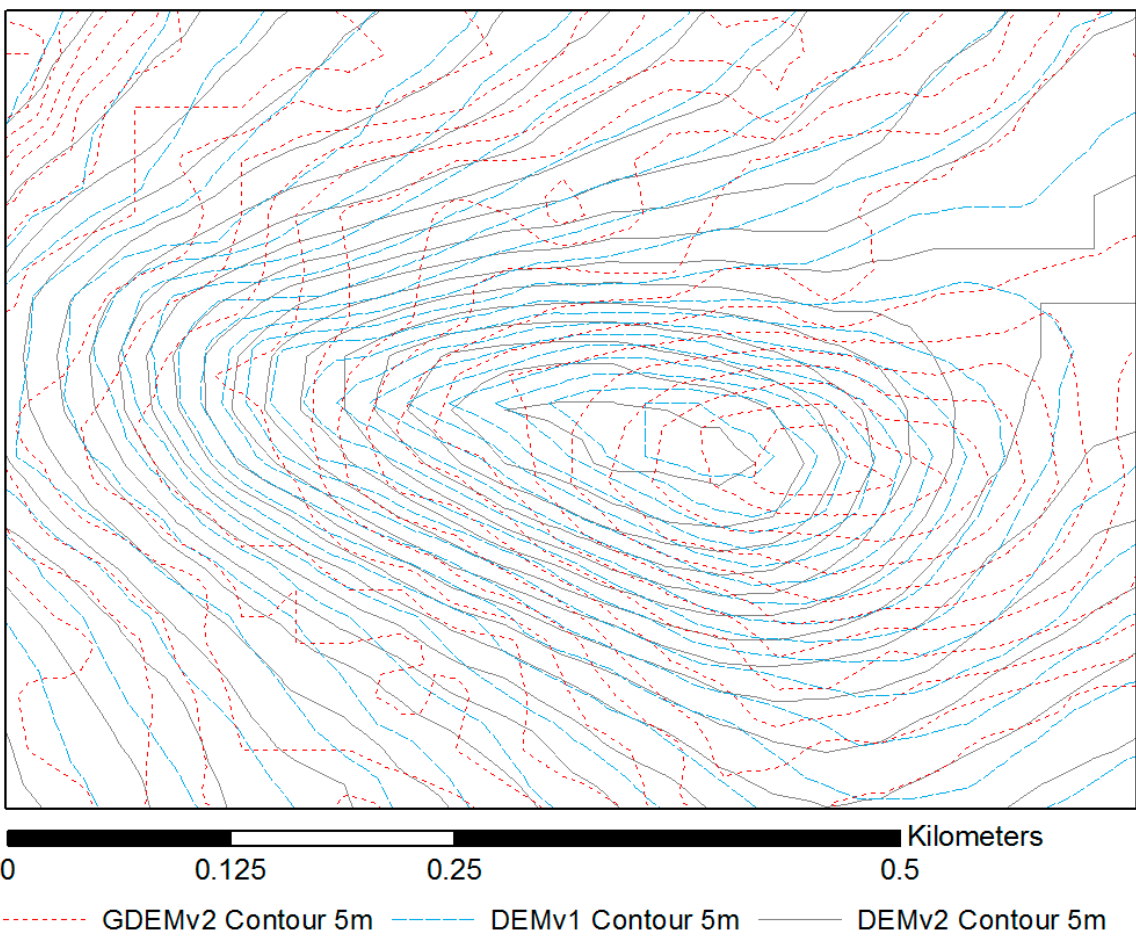


Figure 11. Section of the topographic maps generated from the DEMs

Although the study area's landscape contains an absence of peaks in the southern central region, 37 distinct peaks were identifiable on all three topographic maps (Figure 12). This is an acceptable situation as the data is only subject to interpolation, not warping or other mathematical transformations.

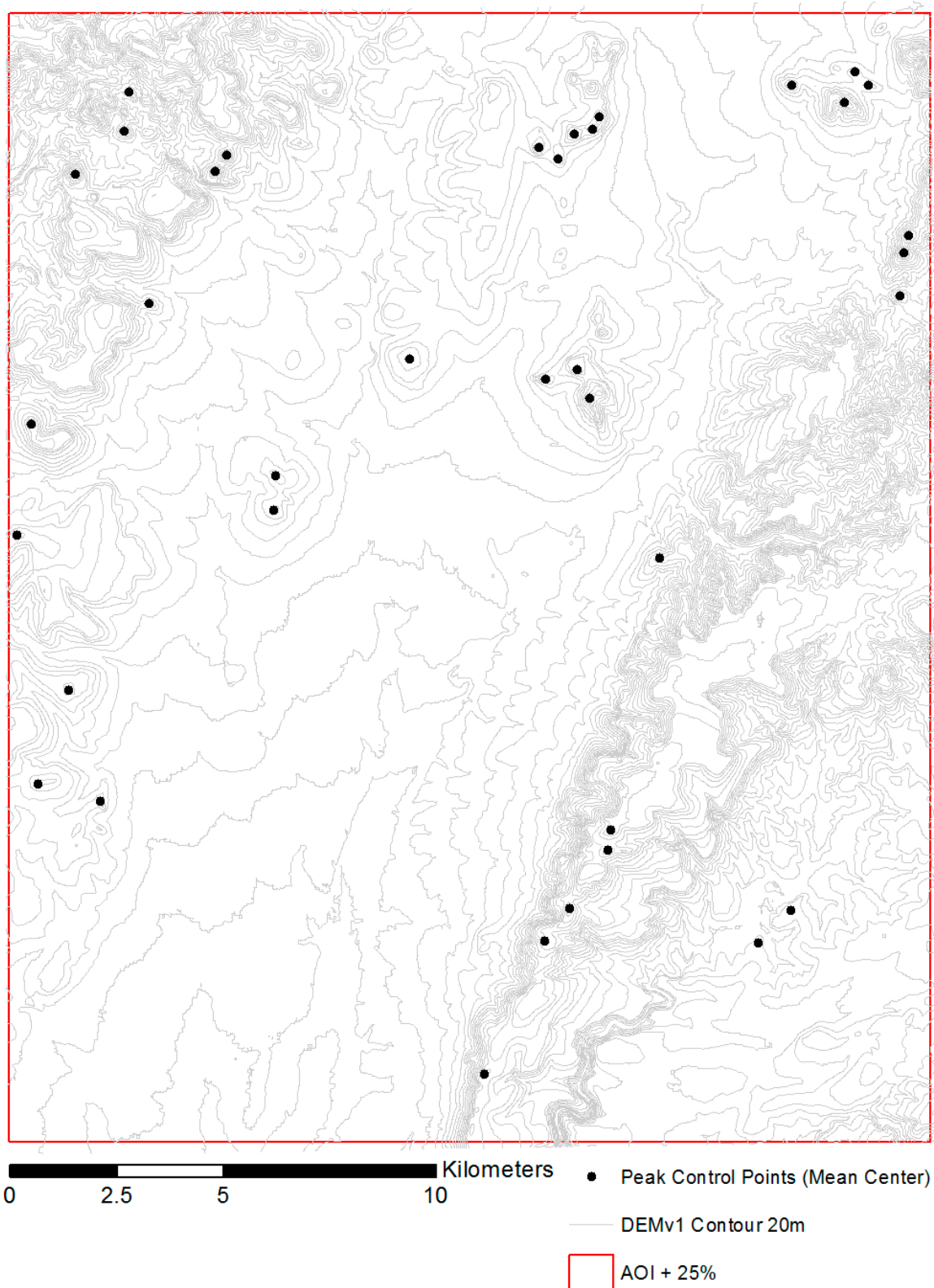


Figure 12. Distribution of peaks used as control points

Identifying the optimal contour line for each peak is difficult to automate, as the identification of lines with the highest elevation value, reflecting the slope of the naturally occurring peak, is a subjective process. For the same reasons as stated above concerning using cell values to determine peak location, the line with the highest elevation value may not represent the peak. Each peak is subject to interpretation. If a peak was uneven or contained multiple peaks, a best-fit or next lower contour line was chosen (Figure 13).

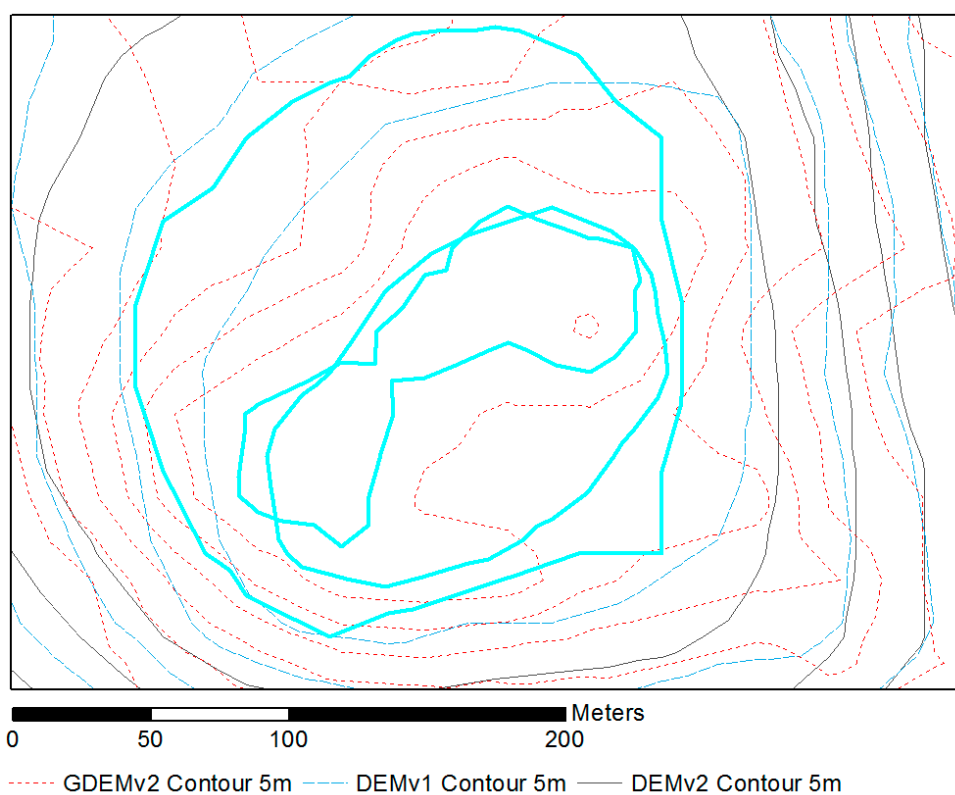


Figure 13. Subjective selection of optimal peak contour lines

Each line's ID was transferred into a data file for automated processing. The data file, in comma separated value (CSV) format, was populated with a header row to identify the DEMs, and subsequent feature ID data (Table 4). Care was taken to ensure that the ID was transcribed without error. Any errors in building the data file results in

erroneous peak point creation, visibly evident when inspecting the results of the process as described below in the next paragraph. A tool, developed in the programming language Python, automates the creation of interpolated peak points. Python was selected as the development language because it is a high-level language, freely distributed, and widely used in the geographic community. The program contains these features:

- 1) Configurable and generic for use in any application
- 2) Automation of many processes, saving time
- 3) Error checking for inconsistencies in the database
- 4) Interpolate peak points for an unlimited number of topographic data sets
- 5) Establish elevation values for the points if the DEM is present

The pseudocode of a software program is a written description of its processes. All mathematical functions and internal procedures and functions are explained using a spoken language. Table 3 contains the pseudocode and full source code is located in Appendix A. The result is a GIS feature class of interpolated peak points and an associated attribute table (Table 4). Viewing the resulting point feature class in ArcMap, the groups of point clusters should be counted and matched against the number of peaks. If the numbers do not match, it is an indication that there may be a typographical error in the database. Mean peak locations for each set of peak points can be generated by ArcMap software using the Spatial Analysis module (Figure 14).

Table 3. Peak Points Interpolation Program - Python Pseudocode

- 0) Define the operational variables required to execute the program.  
 Set Input and Output parameters.  
 Build a list of topographic feature classes and optional DEMs.
- 1) Attempt to open the CSV database file.  
 If the file is not present, warn the user and stop.
- 2) Create an array of GIS layers to store the topographic data files specified in the configuration section of the program.
- 3) For each row of data (IDs) in the CSV database file, perform these functions:
  - Validate the data.
  - If there are errors send a warning message to the operator.
  - If we are on the first (header) row:
    - Save the data
    - End processing for this row (go to Step 3)
  - Select the features in the GIS layers which match the data ( IDs)
  - Convert the selected line features to polygons.
  - Create point(X,Y) features by interpolating the centroid of the polygon features.
  - If the DEM is present, convert the point(X,Y) features to point(X,Y,Z) features
  - Merge all points into a new feature class
  - Add the new feature class name to a master array for final merging after Step 3 is done
  - Remove any extraneous field in the new feature class (clean up)
  - Assign a unique identifier (the row number) to the features in the new feature class
  - Remove any temporary files created in this process
- 4) Create a master feature class by merging all the feature classes contained in the master array, which were created in the previous step
- 5) Add X, Y, (Z if necessary) data values to the master feature class attribute table
- 6) Add an attribute and populate it with the header row data, saved in the previous step, to the appropriate features in the master feature class.
- 7) Remove any temporary files created by the program

Table 4. Input and Output Data of the Peak Points Interpolation Program																																																																																	
CVS Data File Format																																																																																	
gdem_5m,mde1_5m,mde2_5m, 6525,1157,2187, 6346,1137,2011, 6903,1212,2363, ....																																																																																	
Feature Class Attribute Table																																																																																	
<table border="1"> <thead> <tr> <th>FID</th> <th>Shape *</th> <th>Id</th> <th>POINT_X</th> <th>POINT_Y</th> <th>POINT_Z</th> <th>P</th> <th>source</th> </tr> </thead> <tbody> <tr> <td>0</td> <td>Point ZM</td> <td>1</td> <td>722949.454726</td> <td>2486191.47137</td> <td>2152.217681</td> <td>1</td> <td>gdem_5m</td> </tr> <tr> <td>1</td> <td>Point ZM</td> <td>1</td> <td>722886.274165</td> <td>2486204.49183</td> <td>2162.09283</td> <td>1</td> <td>mde1_5m</td> </tr> <tr> <td>2</td> <td>Point ZM</td> <td>1</td> <td>722855.809192</td> <td>2486204.98058</td> <td>2150.725582</td> <td>1</td> <td>mde2_5m</td> </tr> <tr> <td>3</td> <td>Point ZM</td> <td>2</td> <td>723628.205811</td> <td>2486434.4972</td> <td>2206.414191</td> <td>1</td> <td>gdem_5m</td> </tr> <tr> <td>4</td> <td>Point ZM</td> <td>2</td> <td>723623.618085</td> <td>2486417.97089</td> <td>2208.332899</td> <td>1</td> <td>mde1_5m</td> </tr> <tr> <td>5</td> <td>Point ZM</td> <td>2</td> <td>723594.589699</td> <td>2486433.61257</td> <td>2200.741405</td> <td>1</td> <td>mde2_5m</td> </tr> <tr> <td>6</td> <td>Point ZM</td> <td>3</td> <td>723905.501898</td> <td>2485768.57701</td> <td>2249.223029</td> <td>1</td> <td>gdem_5m</td> </tr> <tr> <td>7</td> <td>Point ZM</td> <td>3</td> <td>723931.94639</td> <td>2485755.22303</td> <td>2244.416039</td> <td>1</td> <td>mde1_5m</td> </tr> <tr> <td>8</td> <td>Point ZM</td> <td>3</td> <td>723912.495607</td> <td>2485760.27532</td> <td>2241.395053</td> <td>1</td> <td>mde2_5m</td> </tr> </tbody> </table>		FID	Shape *	Id	POINT_X	POINT_Y	POINT_Z	P	source	0	Point ZM	1	722949.454726	2486191.47137	2152.217681	1	gdem_5m	1	Point ZM	1	722886.274165	2486204.49183	2162.09283	1	mde1_5m	2	Point ZM	1	722855.809192	2486204.98058	2150.725582	1	mde2_5m	3	Point ZM	2	723628.205811	2486434.4972	2206.414191	1	gdem_5m	4	Point ZM	2	723623.618085	2486417.97089	2208.332899	1	mde1_5m	5	Point ZM	2	723594.589699	2486433.61257	2200.741405	1	mde2_5m	6	Point ZM	3	723905.501898	2485768.57701	2249.223029	1	gdem_5m	7	Point ZM	3	723931.94639	2485755.22303	2244.416039	1	mde1_5m	8	Point ZM	3	723912.495607	2485760.27532	2241.395053	1	mde2_5m
FID	Shape *	Id	POINT_X	POINT_Y	POINT_Z	P	source																																																																										
0	Point ZM	1	722949.454726	2486191.47137	2152.217681	1	gdem_5m																																																																										
1	Point ZM	1	722886.274165	2486204.49183	2162.09283	1	mde1_5m																																																																										
2	Point ZM	1	722855.809192	2486204.98058	2150.725582	1	mde2_5m																																																																										
3	Point ZM	2	723628.205811	2486434.4972	2206.414191	1	gdem_5m																																																																										
4	Point ZM	2	723623.618085	2486417.97089	2208.332899	1	mde1_5m																																																																										
5	Point ZM	2	723594.589699	2486433.61257	2200.741405	1	mde2_5m																																																																										
6	Point ZM	3	723905.501898	2485768.57701	2249.223029	1	gdem_5m																																																																										
7	Point ZM	3	723931.94639	2485755.22303	2244.416039	1	mde1_5m																																																																										
8	Point ZM	3	723912.495607	2485760.27532	2241.395053	1	mde2_5m																																																																										
*Id represents the CVS Data File input row number																																																																																	

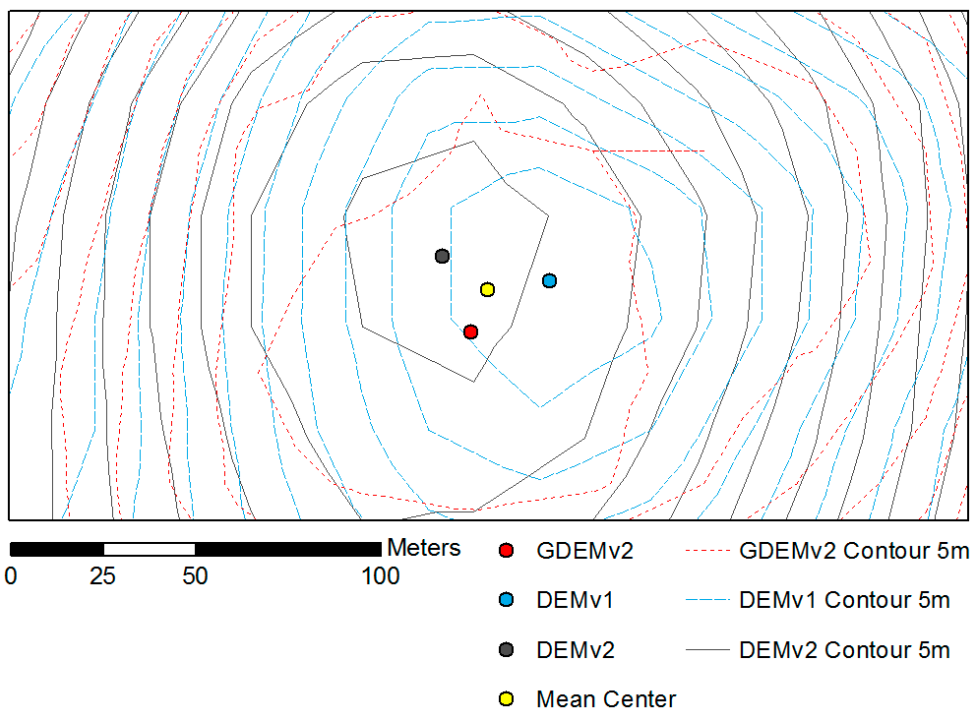


Figure 14. Mean peak locations generated from interpolated peak sets

Spatial analysis of the three peaks' standard distance, the degree to which features are clustered or dispersed around the mean, results in a mean of 21.35 meters, with a range of 9.98 to 39.50, and a standard deviation of 7.43 (Figure 15). The mean positional difference, including one standard deviation, is less the common spatial resolution of 30 meters.

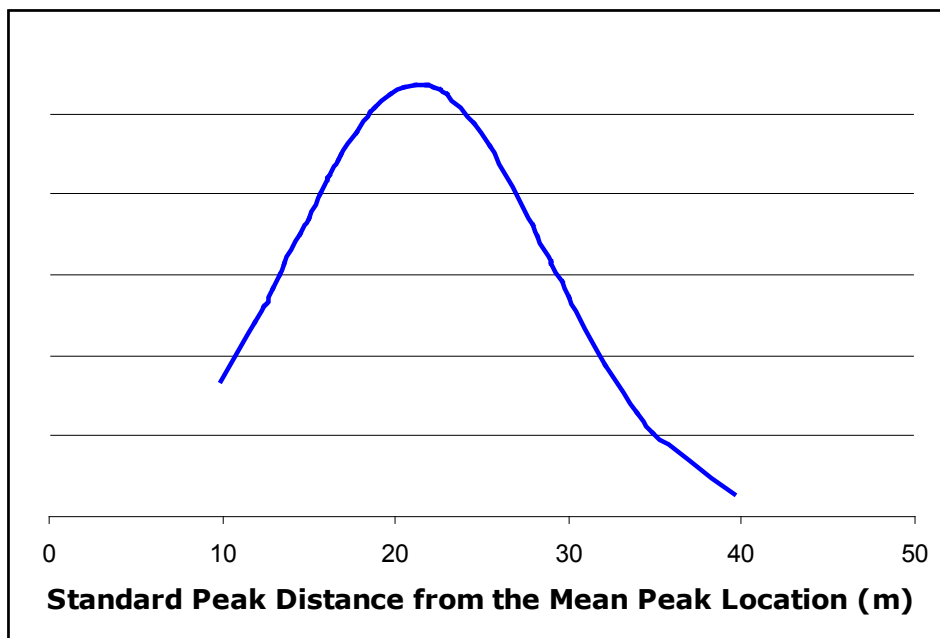


Figure 15. Distribution of standard peak distance of the DEM control point sets

Focusing on the two DEMs from INEGI, if the distance and direction between the peak points is systematic or local patterns appear, that would support the hypothesis that they share a common source. ArcMap does not contain a spatial analysis tool to calculate distance and azimuth between two points. It does have the ability to create a line feature from two points, to which length is an attribute. Using the peak points generated from the previous program, only the points associated with the two INEGI DEMs were selected. Then, the ArcMap tool Points to Line was run, producing a new feature class of lines representing the distance and direction between the peaks. A small python program was

developed to analyze these lines, determine the azimuth, and add data to the line feature attribute table in GIS. The azimuth of two points is a trigonometric function, defined as:

$$\text{Azimuth} = \text{degree} (\arctangent ( \Delta Y / \Delta X ) )$$

The source code to the Azimuth program is located in Appendix B. The program adds azimuth, rounded to the nearest degree, change in X (meters), and change in Y (meters) to each line feature. For the entire area, the mean distance between peaks is 27.90 meters, with a range of 4.93 to 59.78, with a standard deviation of 11.78 (Figure 16).

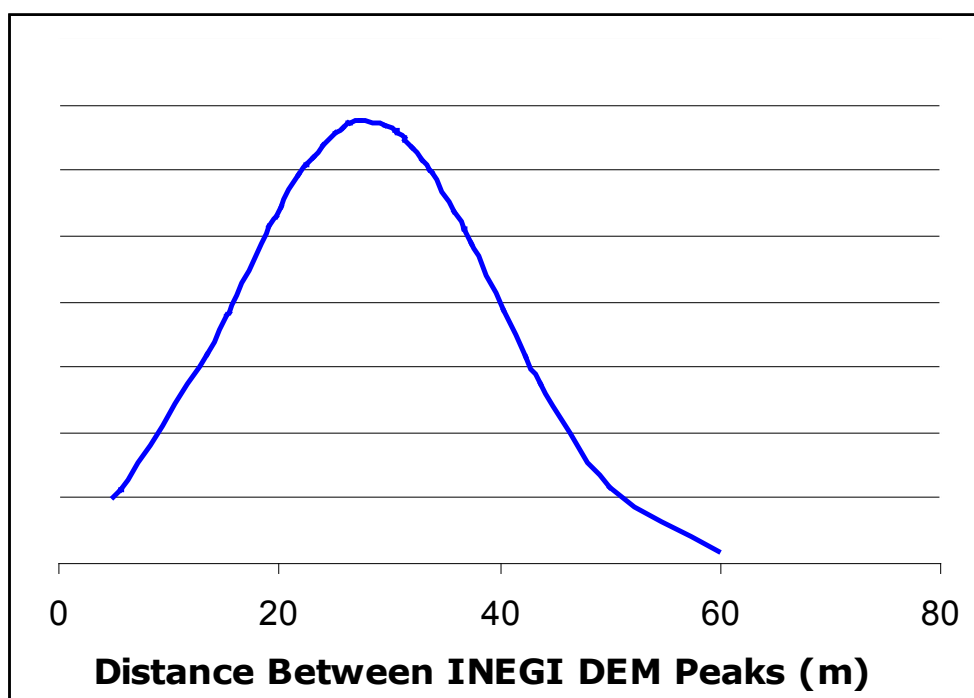


Figure 16. Distribution of distance of the sets of INEGI DEM control points

Figure 17 represents the distribution of azimuth, which indicates that there exists a systematic positional shift in direction to the northwest between version 1 and 2.

Therefore, it is not necessary to assess localized direction values.

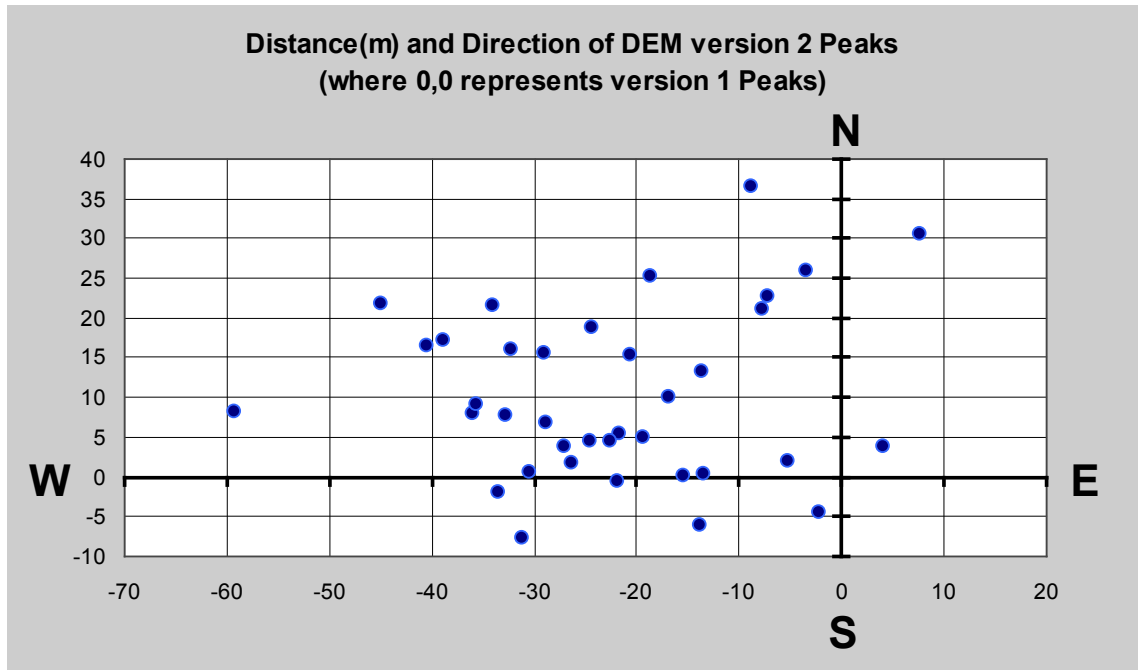


Figure 17. Scatter Plot of the sets of INEGI DEM control points

The presence of a systematic difference in distance and direction between the two DEMs supports my hypothesis that the DEMs are generated from the same source. Based on previous observations listed below, INEGI's DEM version 1 will be used as the target for establishing GCPs on peaks:

- 1) Version 1's artifacts have a local, limited potential to affect accuracy
- 2) Many sinks are present throughout the valley in version 2
- 3) A low mean positional difference of < 30 meters between versions 1 and 2
- 4) Consideration that version 1 is temporally closer in chronometric history to the 1974 survey map
- 5) The interpolated surface of version 1 provides an optimal terrain to identify potential GCPs, compared to GDEMv2's irregular terrain
- 6) The GDEMv2 has a published horizontal accuracy, but the difference has been shown to be negligible, less than one pixel resolution,

These observations do not prove that version 1 is higher in spatial accuracy than the other two, but they do indicate that version 1 is relatively more acceptable to use in this specific study. However, if in validation, a systematic difference between the geo-rectified ASL and the GPS recorded location mimics the systematic difference between the INEGI DEMs, it is reasonable to conclude that replacing version 1 with version 2 will improve overall performance in geo-rectification.

### Approach and Objectives

Multiple approaches to GCP pair selection, including circle and points (Guo 2006), graticule (Rus et al. 2010), and well-distributed (Shaker et al. 2005), resulted in an acceptable degree of resemblance between control point pairs. Circle and points sounds promising, considering the dominant socio-economic site of La Quemada, located in the central portion of the study area, would serve as an excellent origin of the circle with additional ASLs serving as points. This approach is best suited for geo-rectifying oblique distortions by using control points along a centric ellipse. As previously discussed, the historical analysis of the 1974 survey map indicated that it is hand drawn, based on ortho-imagery. The manual cartographic technologies used to create and populate with ASL marks the 1974 survey map may result in random distortion based on human error. Radial distortion inherent in the ortho-imagery used as a reference during the development of the 1974 survey map indicates that oblique distortion most likely does not exist.

Concerning the use of the graticule as a source of GCPs, the previous map assessment concluded that dimensional attributes for the graticule could not be established, negating its potential as a viable approach. Following Shaker et al.'s (2005)

work, a well-distributed approach to establishing GCP pairs will be used in this study.

Principle objectives of establishing sets of GCPs include:

- 1) enough suitable locations ( $n$ ) to satisfy polynomial model order number ( $p$ ).
- 2) evenly distributed across the entire map
- 3) void of linearity and clustering

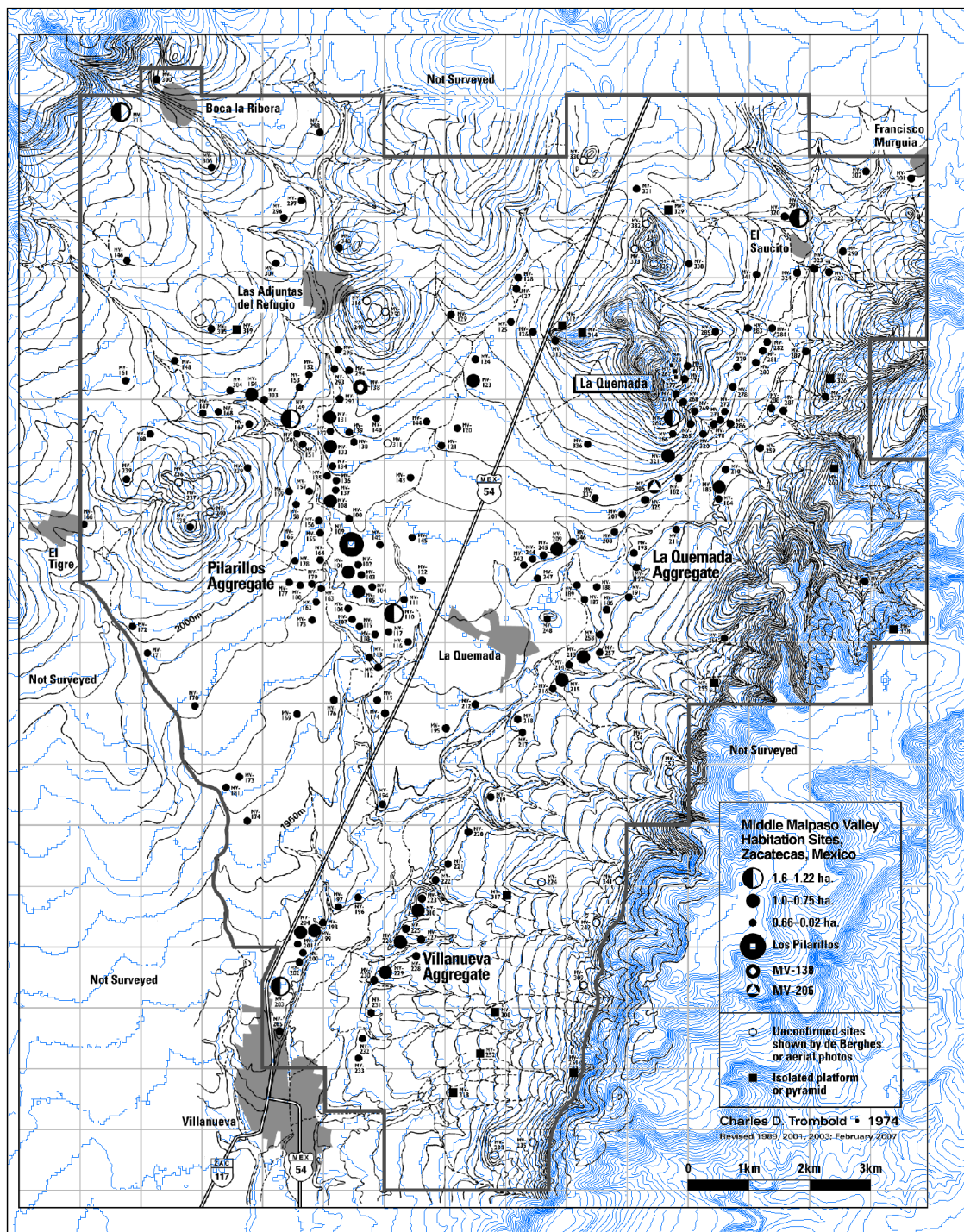
This work subjects the GCPs to ESRI's Warp tool in performing the geometric transformation. The minimum number of GCPs defined by ESRI (2012) to satisfy model operation requirements for orders 1st, 2nd and 3rd is defined as:

$$n = (p + 1) (p + 2) / 2$$

Previous research recommends at least 6 to 28 GCPs for first- and second-order polynomial transformations, and upwards of 40 for third-order polynomial transformation (Shaker et al. 2005; Afify and Zhang 2008). For this work, an attempt will be made to establish as many control point pairs as is possible given the study area's landscape and limited useable features on the 1974 survey map.

### Process and Results

The first task in creating GCPs is to bring the target data files into GIS software and then overlay the historic map using the targets as a guide. Figure 18 shows the 1974 survey map in digital form overlaying a 10-meter topographic map, interpolated from the DEM version 1. This creates an environment that facilitates the process of identifying GCPs on terrain feature locations shared between the historic map and the target data. For peaks, the previously generated interpolated peak point features provide exact directional attributes, while the other GCP point locations were generated by estimation based interpretation of the contour lines and river features.



0 2 4 8 Kilometers  
Figure 18. 1974 survey map fit to display

A rigorous GCP identification and creation campaign resulted in 48 well-distributed GCP pairs (Figure 19). A 5-meter contour data set, interpolated from the INEGI DEM version 1, served as the target for 25 point-pairs. The positional attributes for all 25 points on the topographic map were derived from interpolated peak points generated during the previous DEM analysis and an additional analysis of unique peaks in the study area that were not included in the previous analysis. Of the 25 point-pairs generated on the historic map, well-defined contour line features produced 15, with the additional 10 from abstract lines. A well-defined line formed a closed loop, providing greater confidence in visually interpolating the position of the peak versus abstract lines. Abstract contour lines included line features that insinuated a peak but continued without closure. Twenty-three additional GCP pairs were interpolated from Landsat 5 imagery and the stream network. Of these, 20 were located at stream confluences, while the other three were interpolated at points tangential to bends in the stream features (Table 5).

Table 5. GCP Point Pair Creation Matrix			
Source of Higher Accuracy	GCP Selection Description	1974 survey map Interpolated Feature	# of Points
Topographic map (5m) from DEMv1	Exact coordinates of interpolated peak point feature	Well defined contour line feature	15
		Abstract peak contour line feature	10
Landsat 5 imagery and stream network	Interpolated from pixel values indicating stream presence	Stream confluence feature	20
		Point tangential to bend in stream feature	3
<b>Total</b>			<b>48</b>

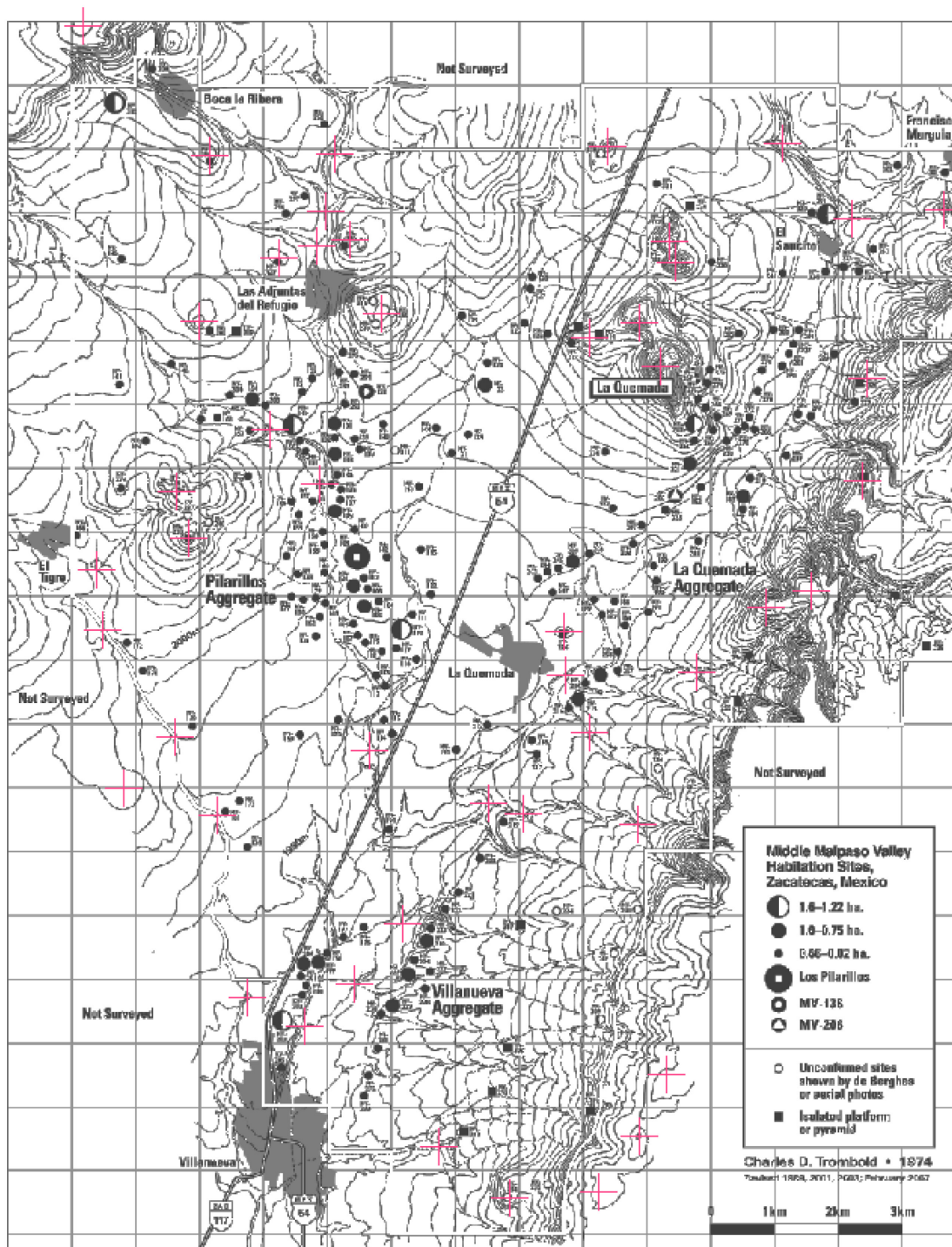


Figure 19. Distribution of the 48 GCPs on the 1974 survey map

## **Geo-rectification**

Having satisfied the minimum number by exceeding the recommended number of GCPs, first-, second-, third-order, adjust and spline polynomial transformations were applied to the 1974 survey map using ESRI's geo-rectification (warp) tool. The warp tool mathematically adjusts the image, based on the control point pairs. First-order, also called affine, performs a shift, rotation and scaling of the map to achieve an overall best-fit to the coordinate space as defined by the targets. The affine model produces a linear distortion, preserving geometric space (Jenny and Hurni 2011). Affine is based on triangulation, therefore, using three control points results in a perfect transformation with a RMSE of 0. With additional control points, residual errors are introduced, with the benefit of an overall better fit to the coordinate space. With an increase in polynomial order to second- and third-, the warp tool achieves greater complexity in distortion, at the cost of a progressive increase in computational demand. Linear distortion is not preserved, producing curved distortions that distribute the error between all control points. The spline model transforms the control points to their exact coordinate space, creating perfect local accuracy, at the cost of unknown accuracy between points. The results of this transformation are residual and RMSE values of 0, necessitating the use of validation points to assess the overall performance of the model. The adjust polynomial model optimizes for a global best-fit to the coordinate space, and then adjusts locally to achieve higher local spatial accuracy. Control points that are within close proximity to each other may compete in the adjust phase, resulting in a failure to achieve a residual value of 0 for all points (ESRI 2012).

After applying a mathematical model, the warp tool applies a resampling algorithm to determine the resulting map's cell values. The resulting map's cell centers often do not line up exactly with the cell centers on the original raster cell, introducing the need to interpolate the value from local values. The nearest neighbor method was chosen as an appropriate resampling algorithm. This method quickly and accurately determines the new cell values based on the cell closest to the new cell's center. This produces the least amount of distortion compared to other algorithms, when applied to categorical data (ESRI 2012). The 1974 survey map is categorical in the sense that it is grayscale, comprised of black, gray, and white cells. A small program in Python executed the five transformation models. The program was no more complex than ESRI's warp documentation. Having originally anticipated multiple GCP selection methods, resulting in multiple sets of control points, requiring multiple sets of transformations models, automating the process of geo-rectification through Python would have introduced multiple benefits. Executing ESRI's geo-rectification tool in Python provides a computational environment with less overhead than executing the tool in ArcGIS Desktop. Due to this work's identification of only one GCP selection process, this benefit of using Python was greatly reduced. However, the ability to automate the generation all five geo-rectified maps and graticule images without supervision, in less time than it took to sequester a cup of coffee was nice. Table 6 outlines the residual values of each transformation model and the RMSE as reported by ArcGIS Desktop. Spline was omitted from the table due to its 0 residual and RMSE values.

Table 6. Geo-Rectification Polynomial Transformation Report				
Control Point	Residual Value (in meters)			
	1st-Order	2nd-Order	3rd-Order	Adjust
1	125.54050	98.13605	101.56866	0
2	79.55094	61.81339	45.06007	0
3	21.58475	22.69404	17.51521	0
4	45.80843	31.95553	38.70056	0
5	11.27310	36.32160	45.10357	0
6	45.45941	76.69200	32.67211	32.67211
7	51.61321	51.55366	44.12358	0
8	47.25352	30.07782	18.10454	0
9	39.44462	37.44116	45.65314	0
10	35.66385	18.76811	30.43076	0
11	49.39369	50.57582	37.56462	0
12	20.86607	27.70495	14.70106	0
13	36.84970	45.48973	29.94080	0
14	14.38390	18.98268	1.46001	0
15	14.54053	26.64179	25.82557	0
16	122.51320	145.83797	142.66377	0
17	27.68637	10.29048	17.73743	0
18	45.03408	68.60640	62.30839	0
19	122.57668	77.88992	66.39269	0
20	87.19518	55.04009	46.12956	0
21	42.43258	8.10031	20.98908	0
22	35.94935	5.18671	25.58736	0
23	10.98887	61.20853	65.99843	0
24	5.80662	24.56298	31.33045	0
25	50.42749	8.92079	10.64654	0
26	48.06969	38.85441	28.22937	0
27	59.78030	30.52642	18.19161	18.19161
28	42.58796	31.95649	34.43603	0
29	84.14147	56.36855	37.81830	0
30	39.41345	20.40560	34.96754	0
31	73.61507	59.99859	69.82449	0
32	155.26436	131.30893	126.71239	0
33	176.91402	137.89599	126.72247	126.72250
34	14.49379	37.67091	47.96415	0
35	65.15487	40.60753	35.99504	0
36	19.82955	23.22304	33.55423	0
37	30.22322	34.51932	28.84269	28.84269
38	63.58069	58.34547	62.11045	0
39	110.81844	103.5027	108.27436	0
40	42.40782	25.38681	28.06170	0
41	70.53261	60.96142	59.64190	0
42	66.65459	68.93460	76.44128	76.44128
43	2.96801	51.17102	41.13201	0
44	37.09924	29.15686	10.38093	0
45	56.13710	30.91845	31.56068	0
46	15.05653	46.06015	51.93320	0
47	55.55954	44.44907	34.31695	0
48	69.56375	26.49693	25.89312	25.89312
RMSE	66.75833	57.34328	54.76900	22.73150

Large residual values may indicate typographical or creation errors, but a review of the point pairs shows no obvious signs of errors that may have been introduced at inception. The six control points showing residual values in the adjust transformation occur where the model sheared the 1974 survey map to optimize local performance. They

are distributed randomly along the control points located along the north, west, and southern edges of the map's area of interest. The residual value range indicates local variance in the historic map's planimetric accuracy. RMSE serves as a measure to determine the overall accuracy of the process of geo-rectifying the hand-drawn map's cartographic coordinate system to a geographic coordinate system. The small range in RMSE values for the first three polynomial transformations may indicate that the polynomial order is moot. The low value reported by the adjust model is interesting. The RMSE value indicates that the adjust polynomial model results in an overall more accurate geo-rectification than the other three, excluding spline, which will be assessed later in this work. Analyzing local variation and comparing the rectified site locations to GPS data will confirm this.

The five rectified map's relational accuracy can be represented by the mean of local accuracies. A side-by-side comparison of the geo-rectified maps shows slight variation between maps, with all having an overall apparent change in shape. However, on the adjust map, there are shear lines appearing on the top and left side. This may be due to the random distribution of the control points and the localized shift that is performed after the polynomial warp. Comparing a new map's graticule with a fishnet grid helps visualize and analyze the global and local distortion (Figure 20). The mean dimensional attributes at a graticule intersection near the middle of the new maps, west of the town of La Quemada, was used to calculate and create a 1-kilometer fishnet in ArcGIS Desktop. This introduces a central bias in relative accuracy. Taking into consideration that there are no absolute points in which to anchor the historic map, using

the center of the map as a reference point delivers a radial bias, and negates any favoritism to one side of the map.

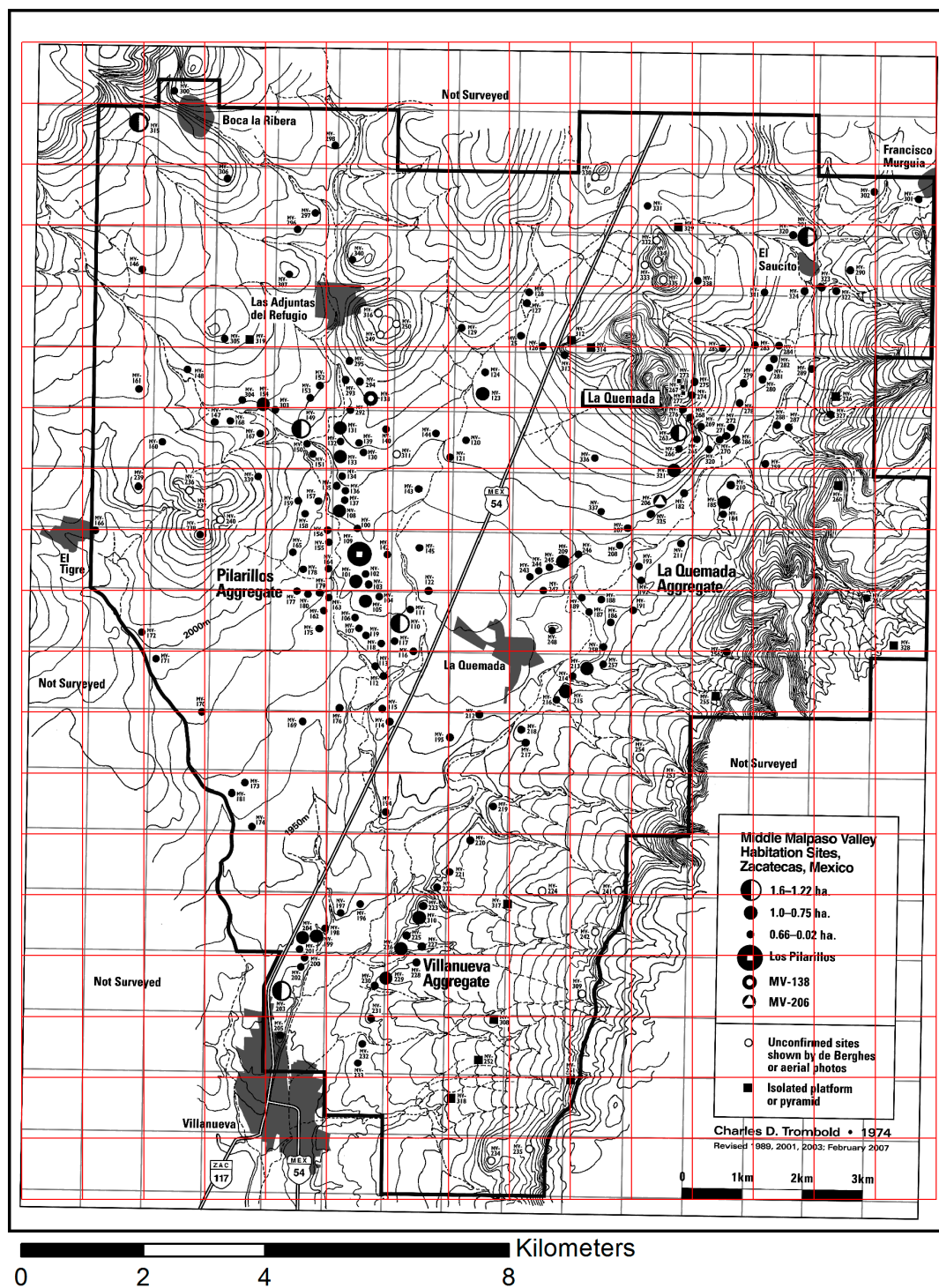


Figure 20. Grid visualizing the distortion in the 1st-order polynomial transformation

In order to partition the survey map into manageable sections, it is necessary to establish a matching grid. Luckily, for this study, the map contains an arbitrary graticule at a 1-kilometer scale. The problem with the graticule is that it is raster format, and cluttered with other map features. Graticules can be digitized with some success, but require complicated software and time (Rus et al. 2010). Adobe Photoshop was used to create a blank image with the exact resolution and size as the digital 1974 survey map. I then transferred the top and left map border to the same position in my new image. After removing contour line features and extending the lines horizontally and vertically, I reproduced the graticule at a 10-pixel width without any other map features. The key in this step was to create a white graticule on a black background due to ArcGIS Desktop's Raster to Polygon working best with background cells containing a value of zero. Subjecting this graticule image to the same geo-rectification transformation as the map resulted in the same positional change. I then used ArcMap Desktop's tool Raster to Polygon to generate vector features mimicking the warped polygons. Using these polygons, the Polygon to Point tool created point features representing the centroids of the polygons. The Spatial Join tool assigned the feature identification number of the fishnet centroids to the five sets of warped centroids. A comparison between each set and the fishnet centroids will result in average localized positional accuracy values for 285 map partitions. The error vectors are too small to visualize across the entire map at print resolution. Figure 21 presents a choropleth map representing the localized mean shift between the 1974 survey map and the maps produced by the four geo-rectification models involving global mathematical functions. Direction vectors are exaggerated for visual purposes.

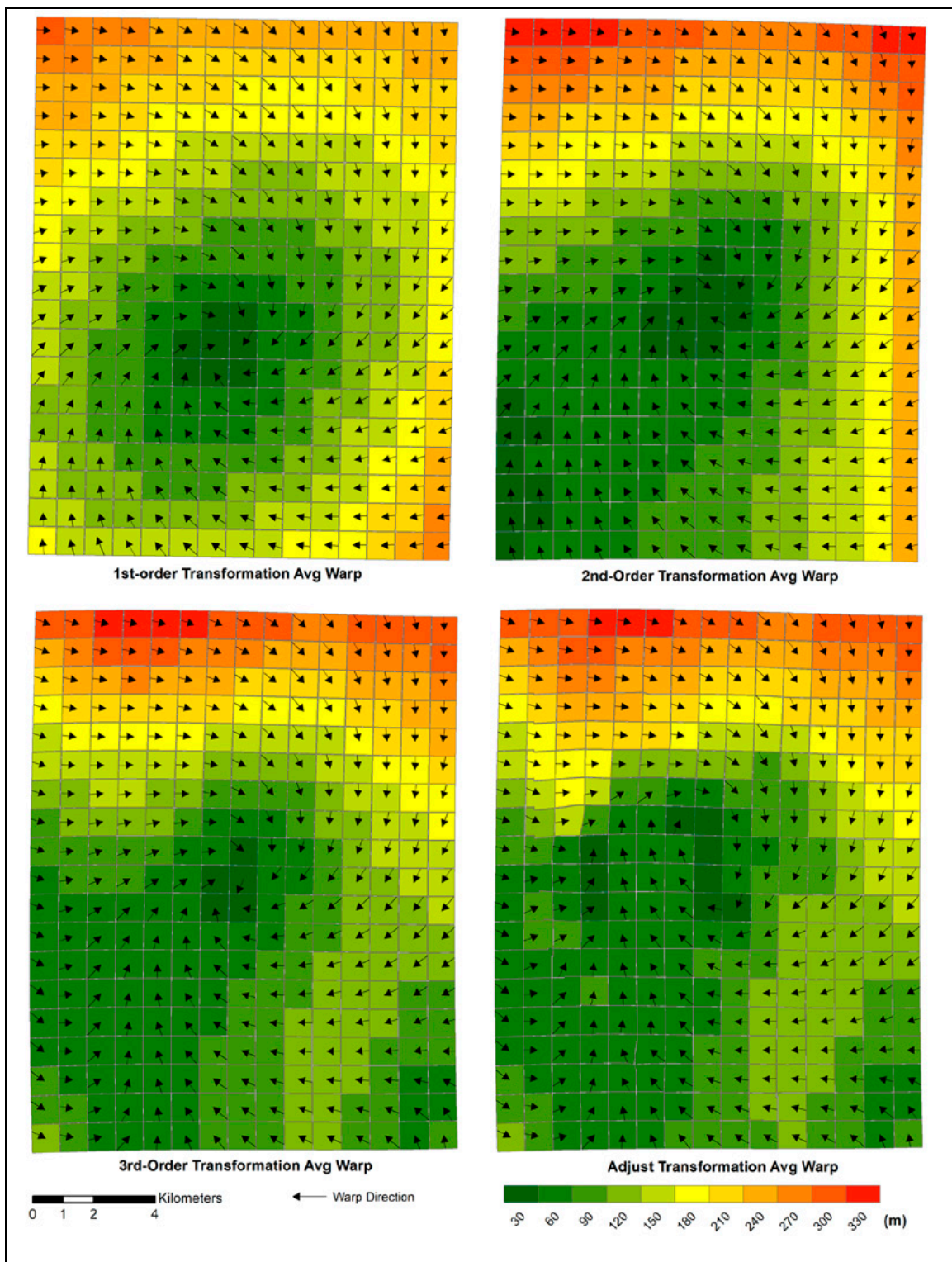


Figure 21. Average cell movement between the 1974 survey map and the rectified maps

Isolating the 183 cells that comprise the survey area as indicated on the 1974 survey map, results in a more accurate analysis of the rectified map's local positional accuracy. The resulting direction vectors (Figure 21) and distribution curves (Figure 22) reflects the complex warping occurring in the higher order polynomial models. This indicates that the second-, third- and adjust polynomial transformations resulted in a similar global transformation, with slightly different results. The mean change in distance varies slightly between the four maps, ranging from adjust at 114 meters and first-order at 117. In combination with the lowest RMSE value, the similar distribution indicates that the adjust transformation provides the best-fit map, compared to the other global warp models.

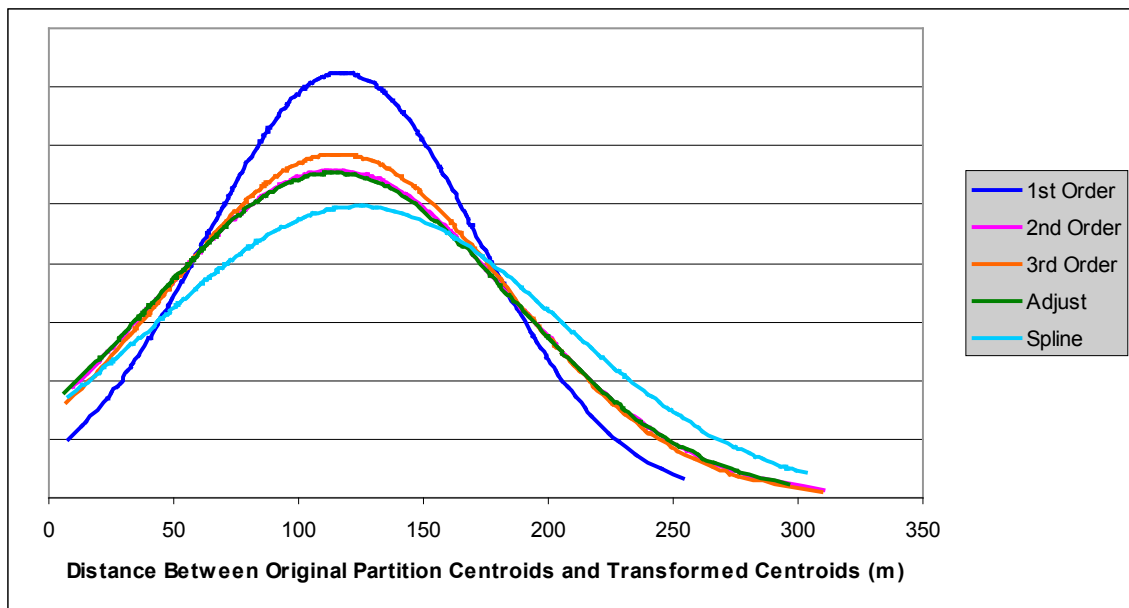


Figure 22. Distribution of localized movement resulting from geo-rectification

Figure 23 presents the localized warping of the local mathematical model, spline. This model resulted in the highest overall warping with a mean cell movement of 124 meters with the largest standard deviation at 80 meters.

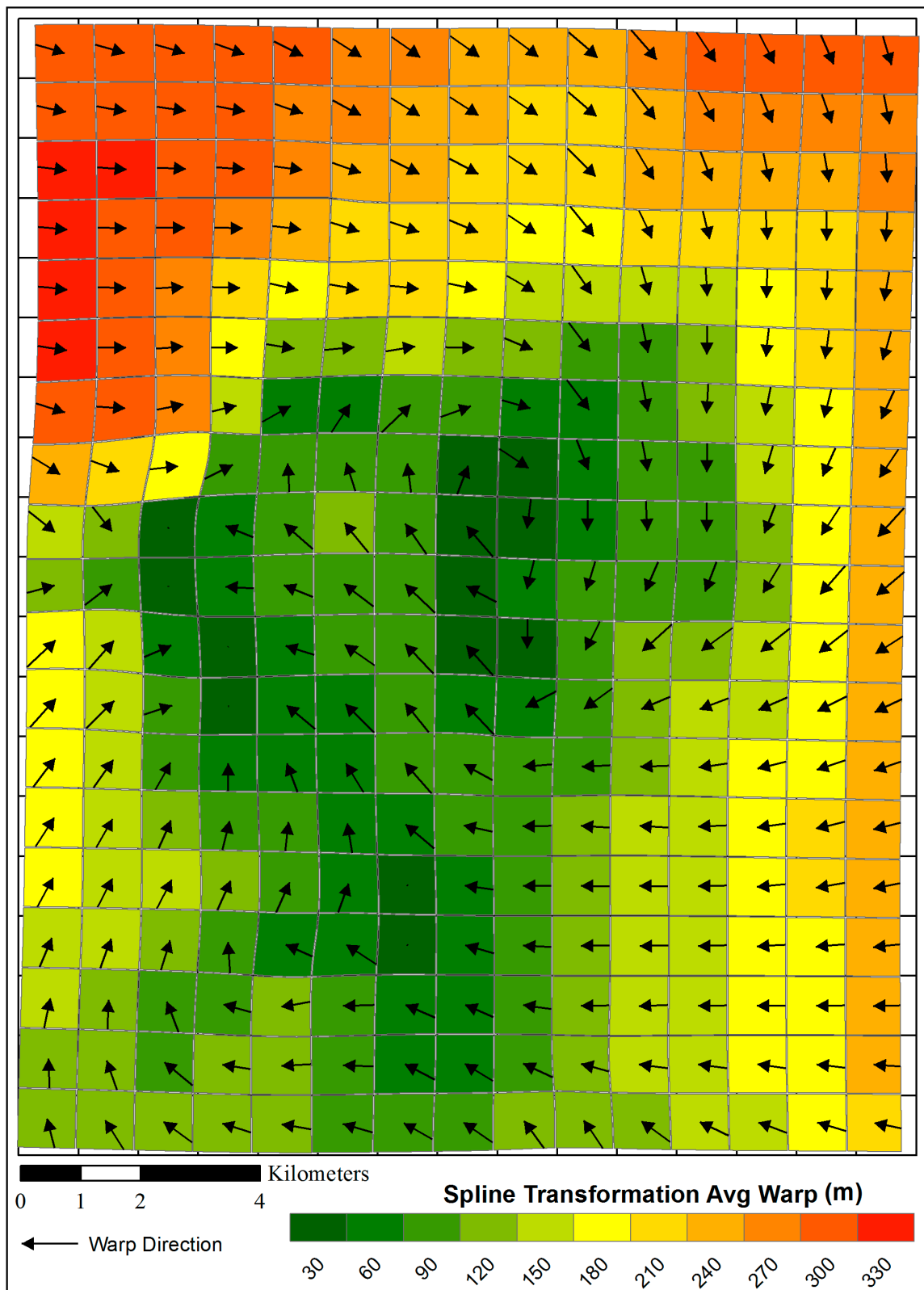


Figure 23. Average cell movement between the 1974 survey map and the spline map

## Validation

Validation will focus on the performances of the adjust and spline geo-rectification model, establish global and local spatial accuracy of the historic map, and provide data to answer the research question if geo-rectification is an alternative method to conducting an additional field survey in order to establish accurate dimensional attributes for the archaeological sites. Analyzing the positional accuracy of the geo-rectified maps requires comparison points with known dimensional attributes. Confidence in the sites' positional attributes, acquired through geo-rectification, can be established by comparing those values to present-day, ground recorded values collected using GPS.

Current handheld GPS units, such as a Trimble, provide sub-meter accuracy in establishing positional data using GPS Differential correction is one method of correcting errors introduced while collecting positional data. A station with a known location routinely collects and calculates positional errors created by GPS satellites and atmospheric conditions. Applying the error values to temporally equal positional data increases the accuracy of the data. While gathering GPS data with devices capable of producing sub-meter accuracy is desirable, it is not always practical. For this limited field work, the combined advantages to using a small handheld: ease of entry through customs, low cost, ease of use in mountainous terrain, and reasonable accuracy, make for a more suitable recording device. A personal hand held GPS receiver (Garmin GPSMap 60CS) satisfied the requirements of this study while providing an acceptable degree of accuracy. Garmin does not publish accuracy reports on their consumer-based GPS products. However, the Garmin 60CS utilizes a built in Wide Area Augmentation System (WAAS), proving improved accuracy from the GPS satellite constellation. The Garmin GPS

receiver automatically selects and applies correction data applicable to the area of operation. These correction data originate from multiple ground stations, and then it is packaged, analyzed, and converted into a master set of correction data. A geo-stationary satellite receives the data set and transmits it down to the receiver in real-time. The handheld unit boasts an achievable +/- 1-meter accuracy, at an unknown confidence level. Analysis of the daily routes taken to and from the field shows excellent precision in the unit's positioning system (Figure 24).

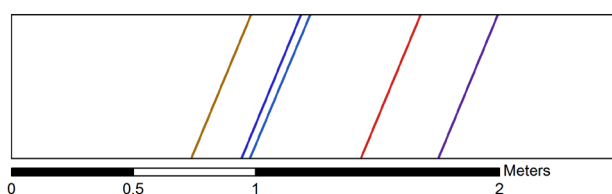


Figure 24. Cross section of Garmin 60CS recordings during five daily excursions

In the summer of 2011, Dr. Trombold and I conducted a limited field survey in the middle Malpaso Valley, with the express goal of collecting positional data for as many archaeological sites that time, weather and logistics permitted. The region's remote location, limited infrastructure development, and a recent increase in private property ownership created barriers while collecting data. In the field, the terrain proved to be extremely inhospitable and difficult to navigate. It was physically impossible to access many of the remote site locations. Hiking to the remote areas in the northwest of the valley required more time than was allotted for this research. In this case, a best attempt was made to acquire as many GPS validation points in unique areas, as possible. Collection began with the northern sites, working back towards the town of Villanueva, which served as base camp. This resulted in a skewed number of GPS readings favoring the northern section of the middle Malpaso Valley compared to the southern part. Five

excursions during a one-week period produced 14 unique routes, resulting in the collection of 40 site location readings (Figure 25).

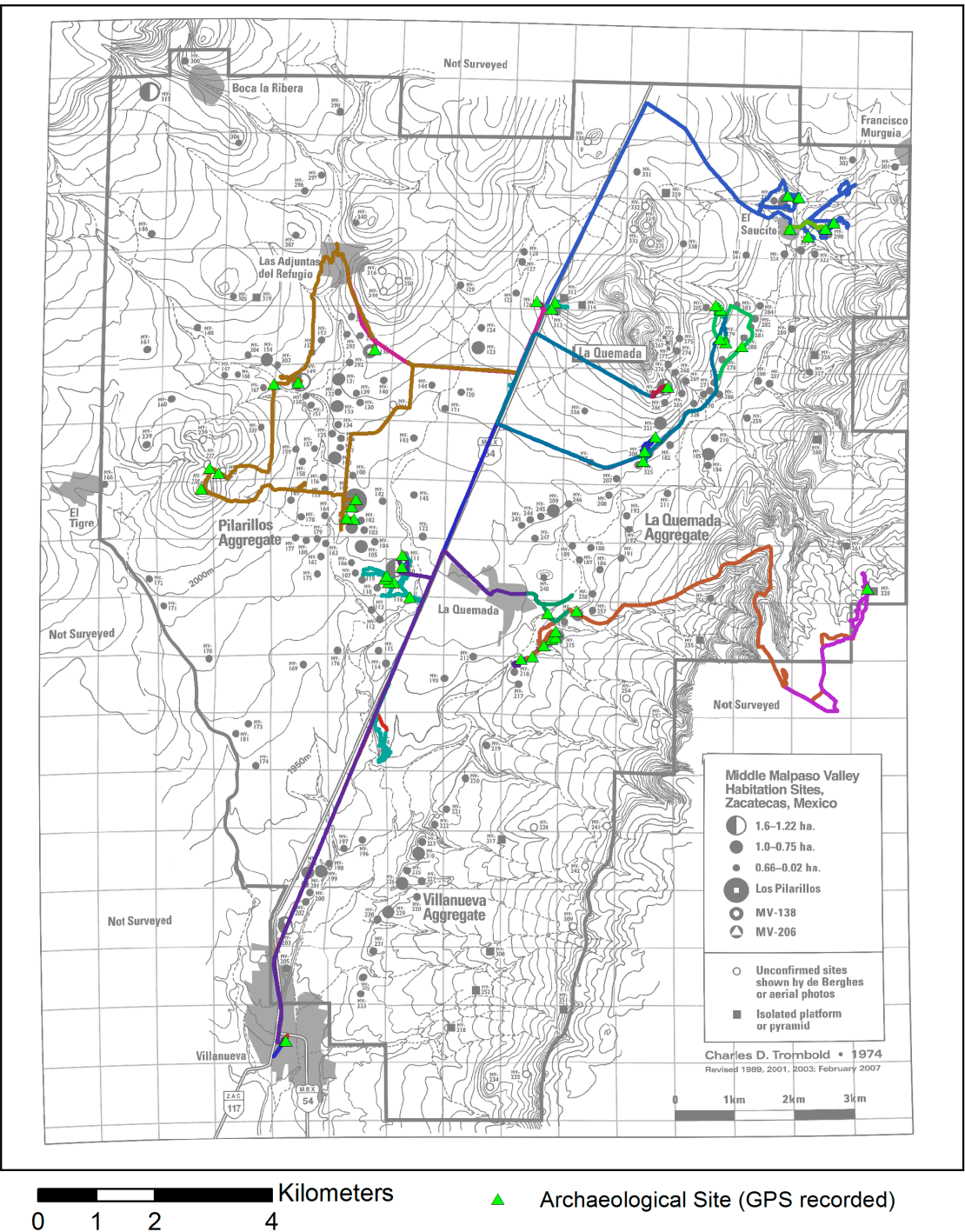


Figure 25. 2011 Limited field survey routes, middle Malpaso Valley, Zacatecas, MX

While conducting the survey, many factors contributed to a potential misappropriation of site number to GPS recording. A temporal period of 37 years between the original and current field survey created a memory vacuum when attempting to locate sites. The valley is saturated with evidence of prehistoric human activity. Except for a few sites, no signs or markings are present to aid in correlating the ruins we encountered to sites marked on the historic map. The survey, based on Trombold's recollection and intuition alone, did not guarantee that the correct site number would be assigned to a GPS recorded location. Unfortunately, this ambiguity in associating the GPS recorded site location to the appropriate site number resulted in the removal of half of the GPS readings. Criteria for removal included: when the GPS location data, thought to be associated with a site, was equidistant or more to another site, and when two or more GPS readings were in close proximity to one site marking (Figure 26).

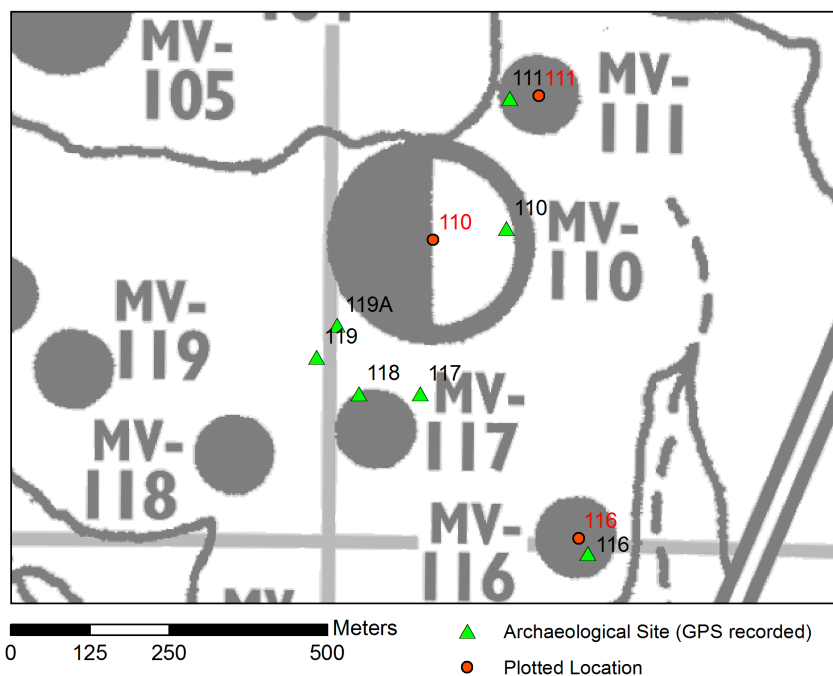


Figure 26. Example of ASL ambiguity between warped map and GPS recordings

Of the 183 surveyed grid cells, 15 contained sites with field collected GPS positional data used in the validation data set (Figure 27). Some of these cells contained multiple points, all of which indicated random distance and direction, highlighting that positional errors were not systematic within each cell.

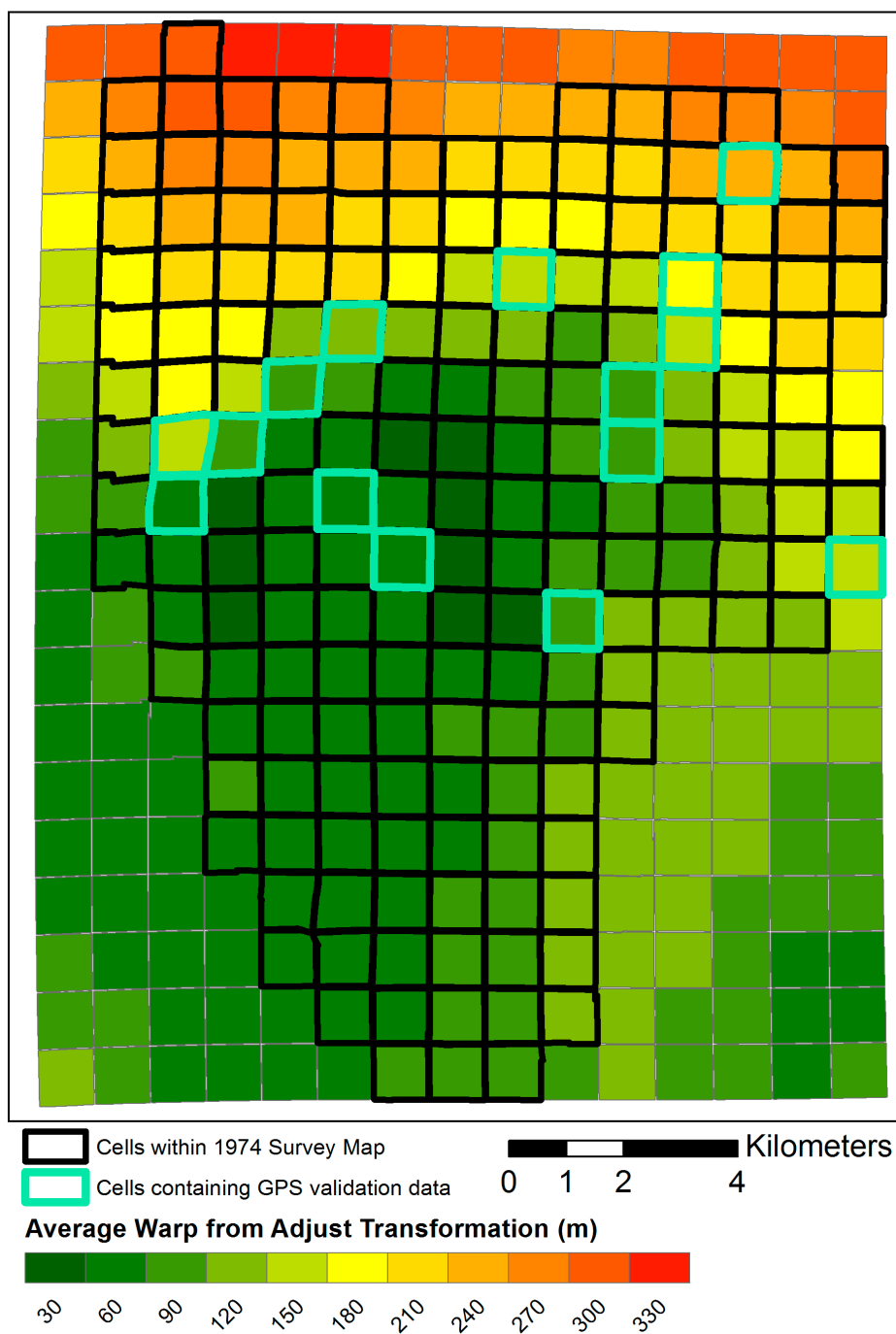


Figure 27. Survey cells with validation data

A new object layer using ArcGIS Desktop was created to record features (points) relating to the geo-rectified site locations that corresponded with a GPS reading. These points were plotted at the visually interpolated centroid of the geo-rectified map's cartographic icon (circle, triangle etc.) used to indicate ASL. Red circles represent the new points in Figure 26. This resulted in five sets of ASLs with dimensional attributes, corresponding to the geo-rectified ASL maps. Analysis the distribution of the positional error between each of the transformations and the GPS collection site locations shows that the adjust model outperformed the other three global models by an average of almost 18 meters. The first- second- and third-order polynomial transformations resulted in similar data sets. Values for each site were within +/- 2 meters and +/- 1 degree of each other (Table 7). Figure 28 plots the distribution, highlighting the random distribution of distance and azimuth.

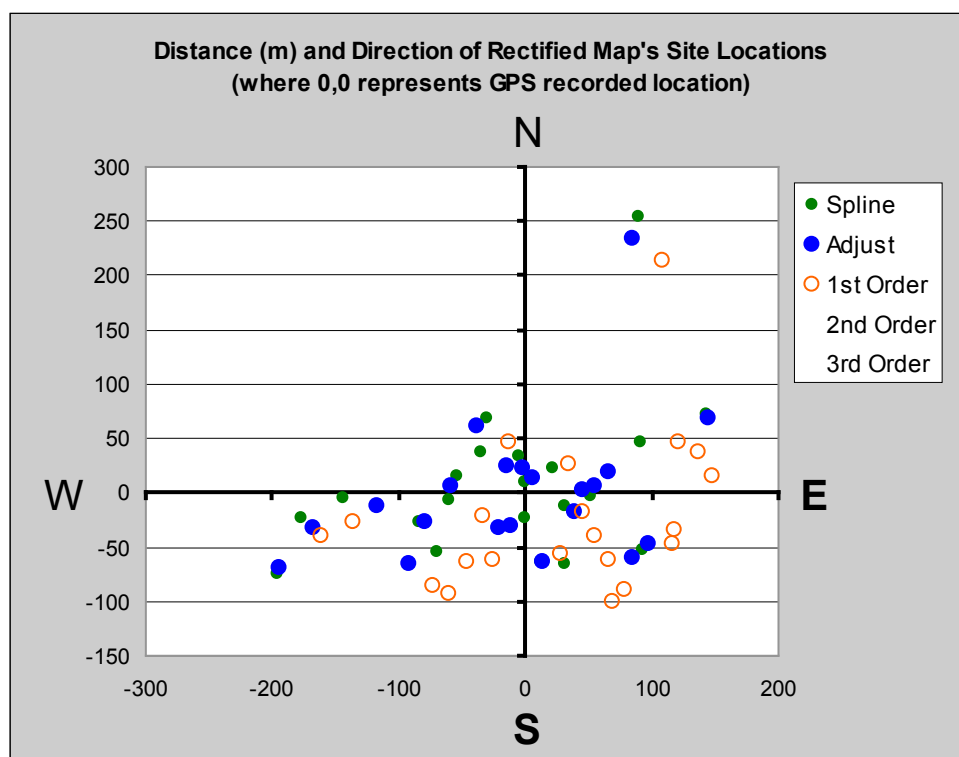


Figure 28. Scatter plot of ASL positional difference

Table 7. GPS to Geo-rectified ASL position						
Site No.	Adjust Transformation		1st-2nd-3rd Order Transformation		Spline Transformation	
	Distance(m)	Azimuth	Distance (+/- 2m)	Azimuth (+/- 1)	Distance(m)	Azimuth
109	38.45	213	123.47	145	60.58	263
110	117.78	263	77.98	217	144.69	268
111	46	87	124.49	112	30.72	43
116	28.55	329	47.92	111	51.61	317
126	31.78	200	66.19	202	23.11	179
138	83.74	251	111.78	213	87.56	251
149	54.94	84	123.38	107	33.66	110
206	43.67	114	69.22	126	52.28	93
213	65.18	167	65.09	153	73.24	154
237	72.42	328	51.81	343	74.02	336
238	14.14	27	128.56	68	9.53	358
240	68.34	74	149.76	84	102.61	62
263	59.24	275	39.93	238	56.09	286
279	21.99	355	42.81	53	34.65	351
285	170.91	259	138.7	259	178.78	262
291	205.41	250	164.78	257	209.45	249
312	159.74	64	141.71	73	160.56	63
313	103.35	125	119.71	139	106.33	119
321	248.97	20	237.48	27	270.10	19
325	111.84	234	112.56	220	89.31	232
328	108.76	115	91.25	131	65.45	168
n=21	Mean = 88.34		Mean = 106 +/-0.2		Mean = 91.16	

The overall rectified site positional error tends to favor the south. Distribution is even to the east and west, indicating no overall systematic error is present in the geo-rectified maps. It is difficult to assess the peak GCP's influence on geo-rectification performance and their relationship to sites use in validation. In a polynomial transformation, the mathematical model is applied continuously to the map. Therefore an even distribution of peak points creates a systematic effect on the positional shift accomplished in geo-rectification. Correcting for version 2's positional shift to the northwest by a mean of 28 meters would not greatly increase overall performance (Figure

17). This indicates that using the INEGI DEM version 2 may not result in a noticeable difference in performance, but does warrant investigation.

Archaeological site size is a factor to consider when assessing the performance of the geo-rectification process as it pertains to ASL positional accuracy. The site size creates a target area, in which any point within the target is sufficient to represent the ASL in spatial analytical methods. The mean archaeological site size recorded during the 1974 survey was 0.39 hectares with a range of 0.10 to 5.12, and a standard deviation of 0.50 (Figure 29). After the 1986 and 2000 field seasons, involving excavations at two of the sites and subsequent field excursions, Trombold concluded that the values recorded in 1974 concerning estimated site size are likely underestimated (personal communication 2011).

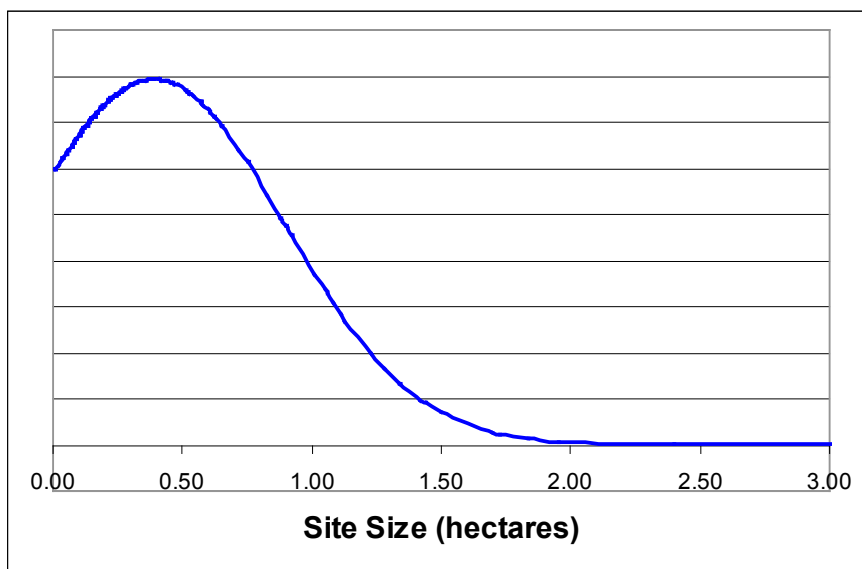


Figure 29. Distribution of 1974 estimation of site size for the middle Malpas Valley

Subtracting a site's radius from the distance between the geo-rectified site mark and the site's GPS recorded position provides a real-world measure of success in using geo-rectification to establish accurate dimensional attributes for sites. Increasing the site

size by an arbitrary value of 15%, to compensate for the likelihood of underestimation, results in a new mean site size of 1.03 hectares and a radius of 47.61 meters for the sites used in validation. Sites 321, 325, and 328 were added after the 1974 field survey, and were assigned a site size based on the average size of the map icon used as indicated on the 1974 map legend. The difference in mean distance reflects the overall performance, and individual distances reflect positional error as a measure of localized performance (Table 8).

Table 8. Consideration of site size in geo-rectification performance								
Site (1974 est.) + 15%			Adjust to GPS (m)		Within?	Spline to GPS		Within?
No.	Size (m <sup>2</sup> )	Radius (m)	Distance (m)	Distance - Radius		Distance (m)	Distance - Radius	
109	58880	136.91	38.45	-98.46	Yes	60.58	-76.33	Yes
110	22425	84.49	117.78	33.29	No	144.69	60.20	No
111	6095	44.05	46.00	1.95	No	30.72	-13.33	Yes
116	2875	30.25	28.55	-1.70	Yes	51.61	21.36	No
126	6555	45.68	31.78	-13.90	Yes	23.11	-22.57	Yes
138	10350	57.40	83.74	26.34	No	87.56	30.16	No
149	27600	93.74	54.94	-38.80	Yes	33.66	-60.07	Yes
206	1955	24.95	43.67	18.72	No	52.28	27.34	No
213	14145	67.10	65.18	-1.92	Yes	73.24	6.13	No
237	2875	30.25	72.42	42.17	No	74.02	43.77	No
238	4485	37.79	14.14	-23.65	Yes	9.53	-28.26	Yes
240	345	10.48	68.34	57.86	No	102.61	92.13	No
263	14720	68.46	59.24	-9.22	Yes	56.09	-12.36	Yes
279	4370	37.30	21.99	-15.31	Yes	34.65	-2.65	Yes
285	3105	31.44	170.91	139.47	No	178.78	147.34	No
291	19895	79.58	205.41	125.83	No	209.45	129.87	No
312	115	6.05	159.74	153.69	No	160.56	154.51	No
313	575	13.53	103.35	89.82	No	106.33	92.80	No
321	10005	56.44	248.97	192.53	No	270.10	213.66	No
325	3910	35.28	111.84	76.56	No	89.31	54.03	No
328	230	8.56	108.76	100.20	No	65.45	56.89	No
Mean	10,262	<b>47.61</b>	<b>88.34</b>		<b>8/21</b>	<b>91.16</b>		<b>7/21</b>

The combination of the global and local warping in the adjust model performed slightly better than the local only spline model. The best mean distance between the

validation sites' ASL map positions produced by the adjust transformation and GPS positions is 88 meters, which is farther than the average site radius of 48 meters, and almost 3 cells (30 m resolution) of the raster data used as the source of higher accuracy.

An analysis of each site provide an explanation to why only eight of the twenty-one validation ASL marks are considered extremely spatially accurate, defined by being located within the site's real-world boundary. While this number may initially appear statistically low, an individual analysis of the sites used in validation shows that the performance of the model is not at fault. Three sites 312, 313, and 325 appear to be intentionally mismarked on the 1974 survey map. They are located adjacent to larger sites, plotting their location would cause an overlap of map symbols. It is possible they were intentionally misplaced in the best interest of the map's intention, to convey the valley's overall site distribution. Sites 285, 291, and 321 are three additional sites that appear to be accidentally mismarked, possibly due to reasons presented in the methodology section. Two other sites, 237 and 240, refer to ASLs indicated on the deBerghes map, but not confirmed during the 1974 field survey. In total, this accounts for positional inaccuracy for eight of the sites used in validation. Four of the remaining five sites are within one pixel's resolution of the estimated site boundary, and may actually be within the site boundary. Personal experience from working at site MV-206 indicates that the site size is grossly underestimated. The GPS recorded site location clearly appears within the site's ASL mark on the geo-rectified map and is an example of an under estimation of the 1974 site size. Site 328 is the only unexplained deviance in model performance.

## CHAPTER VI

### RESULTS AND CONCLUSIONS

#### **Results**

Every prehistoric archaeological site is unique. Size, social use, terrain, biotic community, distance to natural features and other sites, can vary greatly over time and space. Our interpretation of the landscape, and how we choose to represent it on a map, also varies from one individual to another. Dimensional attributes of a site greatly influence positional accuracy on a map. Large sites are more forgiving to a map's spatial accuracy than a small platform or cave feature. Therefore, assessing the positional accuracy of ASLs should be conducted on a localized or case-by-case basis.

In this work, the ASL's total positional error can be represented by function of the total shift in position between the digital 1974 survey map and the GPS recorded position. This research employed a methodology to isolate the total shift in two stages. First, the historic map, through geo-rectification, underwent a global positional shift, resulting in a warped version with a higher degree of spatial accuracy. Localized positional change in the map was isolated in a 1-kilometer grid, providing average values for distance and direction. A high first vector value indicates high potential error in the 1974 survey map. Second, twenty-one sites, with known real-world positional values, provided an additional shift vector. This vector represented the directional change between the geo-rectified site map's ASL, and the ASL's real world coordinates. The

second vector indicates the potential ASL error and or poor GPS data. The total positional error for each site is the hypotenuse of the two vectors. The result reflects localized and infers global spatial accuracy of the 1974 survey map. Table 9 presents an overview of the 21 sites used in validation. The total difference in dimensional attributes of the ASLs, represented by the final distance and azimuth, has a mean of 118 and a range of 5 to 326. Total shift in position was calculated using trigonometric functions to process vector addition, resulting in the total change in X total change in Y, and vector direction. The first few total shifts were calculated by hand, and then an internet-based calculator verified the results and continued to process the data set. The functions used to calculate the distance and angle include:

$$V_a = \sqrt{(V_b^2 + V_c^2 - 2V_bV_c(\cosine \angle A))}$$

$$\Theta = (\arcsine (\sin \angle A * V_{b/c} / V_a))$$

where as :

$V_a$  = vector representing the total positional error

$V_b$  = length of the vector representing the local cell's positional change created by the adjust-polynomial geo-rectification process.

$V_c$  = length of the vector representing the distance between the site's rectified position and the GPS recorded position

$\angle A$  = Angle formed at the union of the end of  $V_b$  and the beginning of  $V_c$

$\Theta$  = Azimuth, adjusted for  $\angle B$ , and using the smaller angle ( $V_b$  or  $V_c$ )

Site No.	1st Vector			2nd Vector		Total Shift in Position			
	CELL	Distance	VectorAz	Distance	VectorAz	$\Delta X$	$\Delta Y$	Distance	Azimuth
109	156	53.8	110.0	38.4	57	3.5	82.6	82.7	1.8
110	142	35.7	133.0	117.8	7	92.7	39.2	100.7	66.4
111	142	35.7	133.0	46.0	183	-70.3	24.1	74.3	288.6
116	142	35.7	133.0	28.6	301	-9.9	1.5	10.0	279.6
126	219	131.6	328.0	31.8	70	122.8	-40.0	129.2	108.0
138	201	118.9	7.0	83.7	19	197.4	40.6	201.5	78.0
149	185	66.8	33.0	54.9	186	1.6	30.8	30.8	2.6
206	176	76.2	269.0	43.7	156	-41.6	-57.8	71.2	215.2
213	130	62.5	236.0	65.2	103	-48.7	12.0	50.2	283.3
237	168	135.0	10.0	72.4	302	171.2	-38.3	175.4	102.5
238	153	35.8	343.0	14.1	243	27.7	-23.3	36.2	129.7
240	169	68.9	20.0	68.3	196	-1.0	5.2	5.3	348.6

263	191	82.7	276.0	59.2	355	66.7	-88.4	110.7	142.3
279	207	127.6	271.0	22.0	275	2.9	-149.5	149.5	178.4
285	222	156.0	279.0	170.9	11	190.3	-121.9	226.0	122.3
291	238	200.9	277.0	205.4	20	215.5	-130.9	252.1	120.7
312	219	131.6	328.0	159.7	206	-32.8	-138.3	142.1	192.9
313	219	131.6	328.0	103.4	145	27.0	-10.3	28.9	111.2
321	191	82.7	276.0	249.0	250	-77.8	-316.1	325.6	193.6
325	176	76.2	269.0	111.8	36	89.1	-11.2	89.8	96.7
328	150	136.6	236.0	108.8	155	-175.4	-65.4	187.2	249.0

\*Vector Azimuth is 0deg at direct E, counting counterclockwise. N=90 W=180 S=270

\*Total Shift in Position Difference +/- 1m due to rounding

Site MV-109, named Los Pilarillos, is a well-known archaeological site in the valley and has the largest estimated site size (5.12 hectares) of all validation sites.

Positional accuracy is very high and we were extremely confident in associating the site number. The ASL mark on the 1974 survey map, the geo-rectified location and the GPS recorded position are all within a margin of error smaller than the site radius of 128 meters, therefore this site has excellent positional accuracy.

Sites MV-110 and MV-111 are located in a barren field, once used as grazing land. MV-110 is a large site, consisting of a small mound with a wide scattering of artifacts. MV-111 is a smaller, nearby site situated on a low plateau overlooking a creek. Positional accuracy is high and we were extremely confident in associating the site numbers. In this case, geo-rectification increased the positional accuracy of one, while decreasing the accuracy of the other. The sites may have been slightly mismarked on the historic map, due to the lack of contour line density. Four other GPS readings taken at nearby ruins were not able to be confidently associated with a site.

Site MV-116 is located on a small hill west of the village of La Quemada, on the western side of the major roadway. The ASL mark on the 1974 survey map, the geo-rectified location and the GPS recorded position are all within a margin of error of the

site's estimated radius, therefore this site has excellent positional accuracy. We were extremely confident in associating the site number.

MV-138 is a medium-size site located along the road to Las Adjuntas del Refugio. This site is well known by Dr. Charles Trombold, and therefore, we were extremely confident in associating the site number. Geo-rectification moved the ASL mark on the 1974 map 120 meters east to well within the site's extent, 84 meters directly short of the GPS recorded position, creating a high level of positional accuracy.

Site MV-149 is located in a remote area south of Las Adjuntas. Positional accuracy is very high and we were extremely confident in associating the site number. Geo-rectification warped the ASL mark east 67 meters, while its GPS recorded positional data was 55 meters to the west of its new location, placing it exactly where the 1974 survey map indicated. Warping decreased the positional accuracy, but only slightly. All three positions are within the site's estimated boundary.

Site MV-206 is along a dirt road south of the Ruins of La Quemada. Positional accuracy is extremely high and we were extremely confident in associating the site number. Geo-rectification did increase the positional accuracy by moving the ASL mark south, within 70 meters of the centroid.

Site MV-213 is a large site with a road cut through the middle. Positional accuracy is extremely high and we were extremely confident in associating the site number. The ASL mark on the 1974 survey map, the geo-rectified location and the GPS recorded position are all within a margin of error smaller than the site radius of 67 meters, therefore this site has excellent positional accuracy.

Sites MV-237, MV-238, and MV-240 are distributed among a peak that rises up from the valley floor, midway between the central drainage system and the western bounding plateau. The peak offers a commanding view of the surrounding valley. MV-238 is comprised of small structures, a retaining wall and a low pyramid. Positional accuracy is extremely high and we were extremely confident in associating the site number as it was directly atop the peak. The other two sites appearing on the historic map originated from the C. deBerghes map circa mid-1800s. No evidence of human occupation was apparent at either of the locations; however, both places in which the GPS readings were acquired resembled the original site descriptions. It is highly plausible, considering the topography and location, sites may have once existed at those two locations. The adjust-polynomial transformation model placed the historic map's ASL mark for MV-238 within 35 and the other within about 70 meters of the GPS recorded position. This high level of positional accuracy was most likely due to the use of the hilltop as a GCP. The localized shift performed by the adjust model, after polynomial warping, placed most GCPs at their target location (Table 6).

Site MV-263 is directly to the east of La Quemada's welcome center, this site was easily recognizable on the terrain. Positional accuracy is extremely high and we were extremely confident in associating the site number. Geo-rectification did increase the positional accuracy by moving the ASL mark south, within 60 meters of the centroid.

Site MV-279 is south of a dirt road, within the terraces associated with the Ruins of La Quemada. Positional accuracy is extremely high and we were extremely confident in associating the site number. Geo-rectification moved the ASL mark on the 1974 map

127 meters due south to well within the site's extent, 20 meters directly short of the GPS recorded position.

Site MV-285 is slightly away from the terrace system of La Quemada. Positional accuracy is medium. The GPS reading is closest to site 285. Confidence is high that we were at the site indicated, but not at the centroid. We may have been at the fringe of MV-285 or a small settlement associated with the site. Due to the dispersion of ruins over a large area and the gently sloping terrain, the site may have been incorrectly positioned on the 1974 Map. Geo-rectification moved the ASL mark south to where it may be, but GPS recorded it 170 meters to the east.

Site MV-291 is a large site located atop a bluff overlooking the confluences of four streams. Positional accuracy is medium and we were extremely confident in associating the site number. The position of the GPS reading is highly accurate with the contour lines of the geo-rectified map. It is possible that the ASL mark was incorrectly plotted and the GPS reading was not at the center of the site. Another GPS reading was taken at what was thought to have been the adjacent site MV-320. That reading fell within the boundary of MV-291, creating ambiguity in association and was therefore not included in this analysis. Although the geo-rectified ASL position is 200 meters away from the GPS reading, it is within an acceptable accuracy due to the site's large size, underestimated in 1974 as 1.73 hectares with a site radius of 74 meters.

Sites MV-126, MV-312, and MV-313 are clustered on the western slope of the mountain in which La Quemada was constructed on and are easily accessed from the major roadway. MV-126 is a small site located on a gently sloping plain of nopal cactus and mesquite trees. Positional accuracy is extremely high and we were extremely

confident in associating the site number to this site. Geo-rectification moved the ASL mark within 30 meters of the GPS location, well within the site's radius of 30 meters. MV-313 was located on the eastern side of the roadway atop a small hill. In this instance, the geo-rectification moved the ASL marking away from its GPS recorded position, resulting in medium positional accuracy. This location was most likely recorded correctly due to its close proximity to the roadway, and intersection and its relationship with La Quemada. MV-313 is a small cave in the northwestern hillside of La Quemada. Reaching the cave is a treacherous trek and a steep cliff interferes with achieving a view of the southern horizon, causing poor satellite reception in the GPS unit. Because of the poor reception, the positional accuracy of the GPS unit was lower than normal, creating an environment of medium to low positional accuracy. We were extremely confident in associating the site number to this site as it is the largest and most well-known cave in the immediate area.

Site MV-321 sits nestled among nopal cactus thickets on a gently sloping hillside south of La Quemada. Confidence was extremely high that we were at the site, as Dr. Trombold worked in that area for years, therefore we were extremely confident in associating the site number. The site was incorrectly marked on the historic map. The effects of geo-rectification cannot be assessed due to the gross positional error of 325 meters.

Site MV-325, located 160 meters down slope of MV-206, is potentially part of MV-206. Positional accuracy is high and we were extremely confident in associating the site number. Geo-rectification slightly decreased the positional accuracy in this case, moving the ASL mark away tangentially south.

Site MV-328, an isolated pyramid and associated structures positioned high atop the eastern escarpment overlooks the valley and Ruins of La Quemada. A 5-meter wide stone causeway leads down towards the valley. Positional accuracy is extremely high and we were extremely confident in associating the site number. Geo-rectification moved the ASL mark 120 meters considerably closer to its GPS reading, which was an additional 80 meters to the west.

GPS locations were recorded for sites MV-215 and MV-216, but were not used in the validation. The two sites are located adjacent to each other on the 1974 map. During the 2011 field survey, we noted that they might both be part of a larger site. An initial GPS reading was taken at MV-216, and an additional three as we encountered ruins along the way where MV-216 was marked. Positional accuracy is extremely high for MV-216 and medium for MV-215. While we were extremely confident in associating the site number, the confusion to exactly which reading should serve as the validation position caused them to be excluded from validation. However, they both exhibit a high degree of spatial accuracy between the geo-rectified ASL map and the multiple GPS readings.

Site MV-290 is on a hillside just outside of a small village, El Saucito. This site was not included in the analysis and serves as an example of ambiguity. While in the field, confidence in associating the site number to the GPS reading was medium. Dr. Trombold's memory could not pinpoint the site's location on the landscape. During the course of investigating the hillside, we discovered an isolated ruin, not thought to be associated with MV-290. A GPS reading was collected at the location due to its potential to contain a large platform plaza with sunken courtyard. Geo-rectification may have

moved the ASL mark closer or farther from the true location, depending on which GPS reading best represented the ASL.

## Conclusions

The 1974 survey map, in its original form, does not possess a global high degree of positional accuracy in defining ASL required by spatial analytical methodologies. Application of historical analysis and GISc methodologies, specifically geo-rectification, to the map successfully produced an ASL map with localized degrees of accuracy (Figure 30).

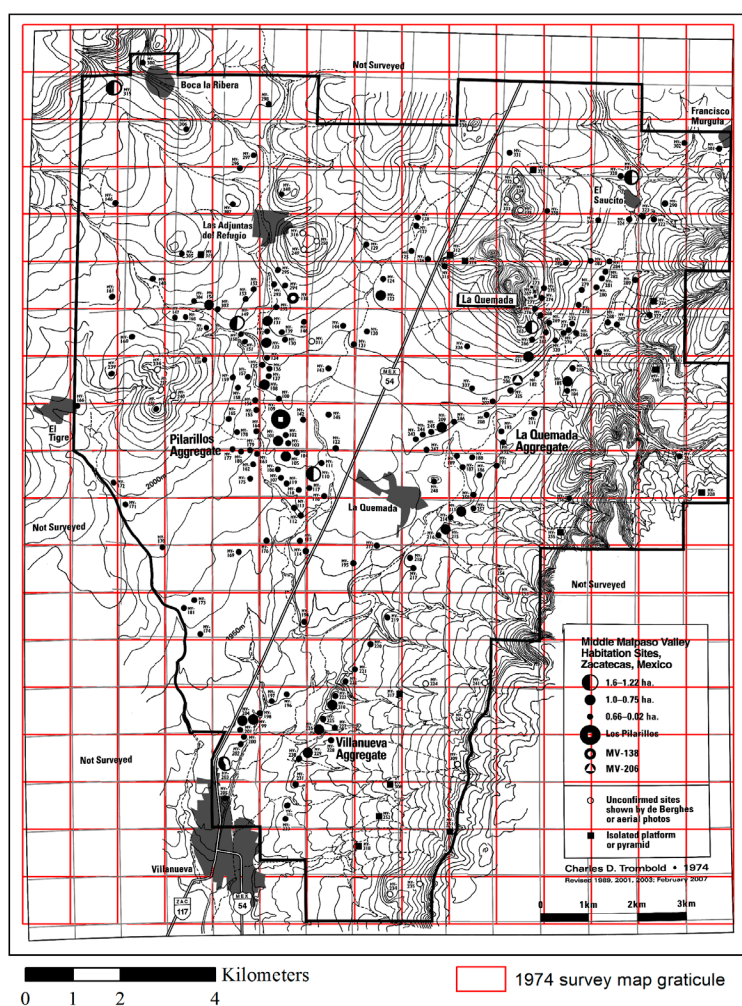


Figure 30. Adjust geo-rectified map produced from the 1974 survey map

This work has shown limited success in establishing positional data for the ASLs in the middle Malpas Valley. The results show that the 1974 survey map is subject to a 'priority placement' scenario, in which large, prominent sites are given optimal placement consideration, while nearby, smaller sites are positioned relatively adjacent in respect to the local, prominent site in so much that no overlapping occurs. The results of this placement methodology results in a high degree of positional accuracy for the site's considered most important to the archaeological record, with diminishing positional accuracy for sites in the surrounding vicinity. This affects the visual representation in site clustering, and may greatly alter results of spatial analysis involving spatial analysis.

The 1974 survey map contained regional variations in positional accuracy. The variation within the map was not systematic. Due to the low (30m) spatial resolution of the source of higher accuracy used to geo-rectify the historic map, the resulting map's overall average positional accuracy reported may not be acceptable for use in some spatial analytical methodologies. An additional GCP selection method based on a systematic, limited field survey, capturing a certain percentage of archaeological site's GPS positional values for site locations may produce a more accurate spatial analysis of the 1974 survey map. Considering Mexico's social and political situation, and the high level of cartel violence, it is not feasible to conduct such a study at this time. Therefore, recommendations include:

- 1) The historic map serves as a general reference for site density and distribution
- 2) Location analysis be limited to the major sites

As highlighted in previous studies, compounding errors in positional accuracy influence the assessment of final map accuracy. Innate errors within the historic map, the

interpolation of target data (DEMs), geo-rectification process, site location creation, and field collected GPS data may have affected the dimensional values. Accuracy of all control points are subjective at best. The resolution of the target and the intermediate-scale of the 1974 map do not lend to the creation of accurate feature locations. Both the historic map and Mexican DEMs are interpolated from topographic maps with an elevation interval of 10 meters. The contour lines themselves were interpolated from interpretation of aerial photography and stereo-pair ortho-imagery (INEGI 2012). These issues can be mediated through the acquisition of higher-resolution raster data or larger-scale maps of the study area.

### **Recommended tasks and additional work regarding improvements**

1) Increase the sample size of the validation set. There is a lack of sites in the southern section of the survey area, which hinders the ability to fully assess the global positional accuracy of geo-rectification. Inclusion of additional sites in the area of interest to achieve an even distribution may show trends in spatial accuracy of the rectified map.

2) Establish positional accuracy values for GPS unit used in this study. Previous analysis of the variance in daily readings shows that the Garmin's precision is adequate for this study. Knowing the horizontal and vertical accuracy of the Garmin, or using a GPS unit with published accuracy will improve the overall confidence in the dimensional data collected in the field.

3) Compare the geo-rectification process in ArcGIS Desktop to other map warping software. MapSource, an open-source software, has been used successfully in other geo-rectification studies.

4) Include an expanded review of Laxton's (1976) discussion on geometric accuracy and Blakemore and Harley's (1980) work concerning aspects of historic map quality, along with a thorough review of related research incorporating GISc. This will enlighten the reader, and provide a better overview of the concepts and applications explored in this work.

5) Develop a GISc tool to automate the performance of multiple sets of geo-rectification models against multiple sets of GCPs. Had this study required the processing of additional sets of GCPs, a tool to automate and utilize multiple-processors would have saved time and an immeasurable amount of sanity.

6) Perform Analysis of Variance (ANOVA) to determine if there are correlations between site attributes and their spatial accuracy on the geo-rectified map. Site size, function, and environmental features may affect ASL positional accuracy.

7) Re-run the geo-rectification using the INEGI DEM version 2 for establishing peak GCP locations to assess any change in geo-rectification performance.

### **Final Comments**

As the implementation of GISc in geography and archaeology increases, the field will benefit from computer programs generated during this research. A robust GISc program to automate the creation of an unlimited number of interpolated peak points, while being generic in nature in order, is applicable in a variety of research situations.

This work paves the way for future work involving GISc in the Malpaso Valley. This research is a technological leap; bringing the original research from the 1970s in line with today's ASL recording methodologies in order to manage existing archaeological

data, conduct complex spatial analysis, and generally promote archaeological endeavors in the area. The results of this work are important components to the future of research in the area. A more robust test of the data generated from this work is highly recommended. In conjunction with environmental data, a model to analyze the ASLs, leading to the creation of a predictability model can be applied to the remainder of the valley and other temporally occupied valleys in the region.

## APPENDIX A

```
# python program to take n topographic shapefiles, and based on user created data
# of peak reference topo line FIDs, generate sets of centroids for analysis of variance
# in interpolated peak location
# by Ryan Schuermann, Summer 2012, rs1571@txstate.edu
print "Initializing modules..."
import arcpy, os
#=====
# BEGIN CONFIGURATION AREA
#=====
#
# root/home directory in which all input/output file locations are based on
#
path= r"E:\geodatabase_MV206"
#
# Output directory/folder - highly recommended to create a unique dir in the
# path directory, and set this variable to it's name... in the case something goes
# wrong, this will make it easier for cleaning up the temp files this program creates
#
outdir = "peak_pts"
#
# Final output shapefile filename
#
OutFname = "Pts_All.shp"
#
# Input file name - text file (.txt/.csv) comma delimited file containing a header row
# and rows of FIDs of peak topo lines for each topo shapefile
#
# data input file format:
# topo1keyword,topo2keyword,topo3keyword,...,
# FID1#,FID2#,FID3#,...,
#
# the first row is a header, used to assign source attribute value
# make sure to end each row with a comma!!
# if the file is not located in path, include the dirs before filename
#
finput = "peak_topo_data.txt"
#
# Array of topo shapefile names,
# MUST BE IN THE SAME ORDER AS HEADER OF finput
# if the topo shapefile is not located in path, include the dir
#
fnameArray=["ASTER_GDEMv2\gdem_utm_contour_5m.shp","INEGI_MDE\mde_utm_contour_5m.shp",
"Zacatecas\zac_utm_contour_5m.shp"]
#
# Interpolate elevation (True/False)?
# If set to True, insert DEM associated with each topo shapefile in demArray,
# following same rules as fnameArray.
```

```

# If set to False, comment out the CheckOut and demArray
#
interpolateElev = True
arcpy.CheckOutExtension("3D")
demArray=["ASTER_GDEMv2\gdem_utm", "INEGI_MDE\mde_utm", "Zacatecas\zac_utm"]

#=====
# END CONFIGURATION AREA
#=====
#
# set variables etc
#
arcpy.env.workspace = path
arcpy.env.overwriteOutput = True
mgmt = arcpy.management
numTopos = len(fnameArray)
message = "Generating peaks for %d topographic shapefiles..." % (numTopos)
print message
#
# open input file for reading
#
try:
    infile = open(os.path.join(path, finput), "r").readlines()
except:
    print "Error: input file not found!!"
    exit()
#
# create an array of layers for each topo shapefile
#
TopoLyr = []
for x in range(numTopos):
    TopoLyr.append(mgmt.MakeFeatureLayer(os.path.join(path, fnameArray[x])))
del x
#
# begin main loop
#
x = 1
myFileArray = []
for row in infile:
    # create an array of values per line
    w = row.split(",")
    # validate and exit if the data row entries do not match number of topo files - user error
    if not(len(w) == numTopos+1):
        errmsg = "Incorrect number of FIDs or missing end comma at input file row %d - %s" % (x, row)
        print errmsg
        exit()
    # get and set vars if on header else process line
    if (x == 1):
        myTopoArray = row.split(",")
        headerLen = 0
        for headerString in myTopoArray:
            if (len(headerString) > headerLen):
                headerLen = len(headerString)
    else:
        # process the topo line files
        myPoly = []

```

```

myPt = []
myInterpPt = []
for y in range(numTopos):
    SQL = "FID = %s" % w[y]
    # select the topo polyline based on FID
    mgmt.SelectLayerByAttribute(TopoLyr[y],"NEW_SELECTION",SQL)
    # create a unique filename for polygon
    myPoly.append(os.path.join(path,outdir,"poly" + str(x-1) + str(y) + ".shp"))
    # create polygon from topo polyline
    mgmt.FeatureToPolygon(TopoLyr[y],myPoly[y])
    # bring in the newly created polygon as a layer
    myPolyLyr = mgmt.MakeFeatureLayer(myPoly[y])
    # create a unique filename for point
    myPt.append(os.path.join(path,outdir,"pt" + str(x-1) + str(y) + ".shp"))
    # create point from polygon
    mgmt.FeatureToPoint(myPolyLyr,myPt[y])
    # interpolate elevation if user defined
    if (interpolateElev):
        # create a unique filename for interpolated point
        myInterpPt.append(os.path.join(path,outdir,"interppt" + str(x-1) + str(y) + ".shp"))
        # interpolate point
        arcpy.InterpolateShape_3d(demArray[y],myPt[y],myInterpPt[y],30,1, \
"NATURAL_NEIGHBORS")

    # merge all
    newout = os.path.join(path,outdir,"pt" + str(x-1) + ".shp")
    if (interpolateElev):
        mgmt.Merge(myInterpPt,newout)
    else:
        mgmt.Merge(myPt,newout)

    # build array of point files to merge at end
    myFileArray.append(newout)

    # remove extraneous fields
    mgmt.DeleteField(newout,"ORIG_FID")

    # set the Id field
    pts = arcpy.UpdateCursor(newout)
    for p in pts:
        p.Id = x-1
        pts.updateRow(p)
    del pts; del p

    # clean up temp files
    for y in range(numTopos):
        mgmt.Delete(myPoly[y])
        mgmt.Delete(myPt[y])
        if (interpolateElev):
            mgmt.Delete(myInterpPt[y])

    # end loop
    outmsg = "Generated centroids for peak %d..." % (x-1)
    print outmsg
    del myPoly; del myPt; del myInterpPt; del newout
# increment loop counter etc

```

```
x += 1
del w

# merge all peak's points
print "Merging all point files..."
finalout = os.path.join(path,outdir,OutFname)
mgmt.Merge(myFileArray,finalout)

# add X,Y and maybe Z data to attribute table
mgmt.AddXY(finalout)

# add an attribute for dem source and populate according to order of merge
mgmt.AddField(finalout,"source","TEXT","",headerLen+1)
del headerLen
print "Populating source field..."
pts = arcpy.UpdateCursor(finalout)
y = 0;
for p in pts:
    p.source = myTopoArray[y]
    y += 1
    if (y == numTopos):
        y = 0
    pts.updateRow(p)
del pts; del p

# clean up temp files
print "Deleting temp files..."
for f in myFileArray:
    mgmt.Delete(os.path.join(path,outdir,f))

print "Done!"
```

## APPENDIX B

```
#####
# Author: Ryan Schuermann
#-----
# Description: a script to get azimuth from a simple line
# Make sure to have a fields called:
#   Azimuth - type Integer
#   diffX and diffY - type Double
# Change srcLyr to your layer name
#####
import math,arcpy
srcLyr = "MdePeakDif"
desc = arcpy.Describe(srcLyr).ShapeFieldName
cur = arcpy.UpdateCursor(srcLyr)
for row in cur:
    feat = row.getValue(desc)
    # gets azimuth from beginning point to end point
    # switch points assignment to get azimuth from last to first point if line is in opposite direction
    fromPt = feat.firstPoint
    toPt = feat.lastPoint
    x1 = fromPt.X
    y1 = fromPt.Y
    x2 = toPt.X
    y2 = toPt.Y
    deltaX=x2-x1
    deltaY=y2-y1
    Az = math.atan(deltaY/deltaX)
    Az = math.degrees(Az)
    if (deltaX < 0):
        Az += 180
    Az = 90 - (Az+180 % 360-180)
    if(Az < 0):
        Az += 360
    row.Azimuth=int(Az)
    row.diffX = deltaX
    row.diffY = deltaY
    cur.updateRow(row)
```

## LITERATURE CITED

- Afify, H. and Y. Zhang. 2008. Accuracy Assessment of User-Derived RFCs for Ortho-Rectification of High-Resolution Satellite Imagery. *International Journal of Geoinformatics*, Vol. 4, 4, 17-24.
- Bancroft, H.H. 1875. *The Native Races of the Pacific States of North America*, D. Appleton and Company, New York, Vol. 4.
- Batres, L. 1903. *Visita a los Monumentos Arqueologicos de La Quemada, Zacatecas, Mexico*. Mexico D. F.
- Benavides, J. and E. Koster. 2006. Identifying Surviving Landmarks on Historical Maps. *e-Perimtron*, Vol. 1, 3, 194-208.
- Black, S.L. and K. Jolly. 2003. *Archaeology by Design (Archaeologist's Toolkit 1)*. Walnut Creek, CA. AltaMira Press.
- Blakemore, M.J. and J.B. Harley. 1980. Concepts in the History of Cartography. A Review and Perspective. *Cartographica*, 17, 1-120.
- Boccardo, P., E.B. Mondino, F.G. Tonolo, and A. Lingua. 2004. Orthorectification of High Resolution Satellite Images. In: Altan, O. (Ed.), *XXth ISPRS Congress, Istanbul, Turkey. Technical Commission I*, 30-55.
- Braun, D.P. and S. Plog. 1982. Evolution of Tribal Social Networks - Theory and Prehistoric North-American Evidence. *American Antiquity*, Vol. 47, 3, 504-525.
- Brůna, V., K. Křováková, and V. Nedbal. 2010. Historical Landscape Structure in the Spring Area of the Blanice River, Southern Bohemia - An Example of the Importance of Old Maps. *Acta Geodaetica et Geophysica Hungarica*, Vol. 45, 1, 48-55.

- Eckert, Max. 1908. On the Nature of Maps and Map Logic. *Bulletin of the American Geographical Society of New York*, Vol. 40, 6, 344-351.
- Elliott, M. 2005. Evaluating Evidence for Warfare and Environmental Stress in Settlement Pattern Data from the Malpaso Valley, Zacatecas, Mexico. *Journal of Anthropological Archaeology*, 24, 297-315.
- Elliott, M., C.T. Fisher, B.A. Nelson, R.S. Molina Garza, S.K. Collins, and D.M. Pearsall. 2010. Climate, Agriculture, and Cycles of Human Occupation Over the Last 4000yr in Southern Zacatecas, Mexico. *Quaternary Research*, 74, 26-35.
- ESRI. 2012. ArcGIS Resource Center: ArcGIS 10.1. Retrieved June 21st, 2012, from <http://resources.arcgis.com/en/help/main/10.1/index.html>
- Federal Geographic Data Committee. (FGDC) 1998. Geospatial Positioning Accuracy Standards Part 3 FGDC-STD-007-1998, Washington, D.C.
- Fogel, D. 1996. Image Rectification with Radial Basis Functions: Application to RS/GIS Data Integration. Paper Presented at the Third International Conference/Workshop on Integrating GIS and Environmental Modeling, NCGIA Publications, University of California, Santa Barbara.
- Gil, M., E. Corbelle, and J. Ortiz. 2011. Orthrectification of Quickbird Ortho-ready Imagery: A case study over mountainous terrain. *Survey Review*, Vol. 43, 320, 199-209.
- Guo, F. 2006. Plane Rectification using a Circle and Points from a Single View. Paper presented at the 18th International Conference on Pattern Recognition. IEEE Computer Society.
- Hers, Areti M. 1989. Los Toltecas en Tierras Chichimecas. UNAM, Instituto de Investigaciones. *Estéticas, cuadernos de historia del arte* 35.
- Hrdlička, Aleš. 1903. The Region of the Ancient "Chichimecs," with Notes on the Tepecanos and the Ruins of La Quemada Mexico. *American Anthropologist, New Series*, Vol. 5, 3, 385-440.

- Hutchinson, M.F., T. Xu, and J.A. Stein. 2011. Recent Progress in the ANUDEM Elevation Gridding Procedure. In: T. Hengel, I.S. Evans, J.P. Wilson and M. Gould (Ed.), *Geomorphometry 2011*, Redlands California, USA, 19-22.
- Ignacio, J. and M. Quintero. 2011. Comentarios Sobre el Patrón de Asentamiento en el Valle del Río Verde-San Pedro (Aguascalientes) Durante el Epiclásico. *TRACE*, Centro de Estudios Mexicanos y Centroamericanos, Vol. 59, 105-121.
- Instituto Nacional de Estadística y Geografía (INEGI). Retrieved March 22nd, 2011 from <http://www.inegi.org.mx/sistemas/mexicocifras/>
- Instituto Nacional de Estadística y Geografía (INEGI). Retrieved May 30th, 2012 from <http://www.inegi.org.mx/geo/contenidos/datosrelieve/continental/continuoelevaciones.aspx>
- Jiménez Betts, P. 1990. Una Red de Interacción del Noroeste de Mesoamérica: una Interpretación. In: Boehm de Lameiras, B. and P. Weigand (Ed.), *Origen y desarrollo de la civilización en el occidente de México*. Centro de Estudios Antropológicos, Colegio de Michoacán, Zamora, Michoacán, Mexico, 1-22.
- Karney, Charles F.F. 2011. Transverse Mercator with an Accuracy of a few Nanometers. *Journal of Geodesy*, Vol. 85, 8, 475-485.
- Kelley, J. Charles. 1971. Archaeology of the Northern Frontier: Zacatecas y Durango. In: Ekholm, G.F. and I. Bernal (Ed.), *Archaeology of Northern Mesoamerica, Part 2. Handbook of Middle American Indians*. University of Texas Press, Austin, Vol. 11, 768-801.
- Kvamme, K.L. 2006. There and Back Again; Revisiting Archaeological Locational Modeling. Paper presented at the GIS and Archaeological Site Location Modeling, 3-38.
- Laxton, P. 1976. The Geodetic and Topographic Evaluation of English County Maps, 1740-1840. *The Cartographic Journal*, 13, 37-54.

- Lockheed Martin Space Operations. 2004. Geopositional Accuracy Validation of Orthorectified Landsat MSS Imagery. Retrieved June 20th, 2012 from [http://ntrs.nasa.gov/archive/nasa/casi.ntrs.nasa.gov/20050160947\\_2005162513.pdf](http://ntrs.nasa.gov/archive/nasa/casi.ntrs.nasa.gov/20050160947_2005162513.pdf)
- McGuire, Randall H., E.C. Adams, B.A. Nelson, and K.A. Spielmann. 1994. Drawing the Southwest to Scale: Perspectives on Macroregional Relations. In: Gumerman, G. (Ed.), *Themes in Southwest Prehistory*. School of American Research Press, Santa Fe, 239-265.
- McRoberts, Ronald E. 2010. The Effects of Rectification and Global Positioning System Errors on Satellite Image-based Estimates of Forest Area. *Remote Sensing of Environment*, Vol. 114, 8, 1710-1717.
- Meyer, D. 2011. ASTER Global Digital Elevation Model Version 2 - Summary of Validation Results. Retrieved March 8th, 2012 from [http://www.jspacesystems.or.jp/ersdac/GDEM/ver2Validation/Summary\\_GDEM2\\_validation\\_report\\_final.pdf](http://www.jspacesystems.or.jp/ersdac/GDEM/ver2Validation/Summary_GDEM2_validation_report_final.pdf)
- Nelson, B.A. 1994. Outposts of Mesoamerican Empire and Architectural Patterning at La Quemada, Zacatecas. In: Wooseley, A. and J. Raveslout (Ed.), *Culture and Contact: Charles C. DiPeso's Gran Chichimeca*. University of New Mexico Press, Albuquerque, 173-190.
- Nelson, B.A. 1995. Complexity, Hierarchy, and Scale: A Controlled Comparison Between Chaco Canyon, New Mexico, and La Quemada, Zacatecas. *American Antiquity*, 60, 587-618.
- Neurath, J. and D. Bahr. 2005. Cosmogonic Myths, Ritual Groups, and Initiation: Toward a New Comparative Ethnology of the Gran Nayar and the Southwest of the US. *Journal of the Southwest*, Vol. 47, 4, 571-614.
- Perry-Castañeda Library Map Collection. 1975. Atlas of Mexico. Retrieved April 29, 2011, from [http://www.lib.utexas.edu/maps/atlas\\_mexico/climate.jpg](http://www.lib.utexas.edu/maps/atlas_mexico/climate.jpg)
- Podobnikar, T. 2010. Historical Maps of Ljubljana for GIS Applications. *Acta Geodaetica et Geophysica Hungarica*, Vol. 45, 1, 80-88.

- Portillo and J.L. Weber. 1935. *la Conquista de la Nueva Galicia*. Talleres Graficos de la Nación, Mexico D. F.
- Rus, I., C. Balint, V. Craciunescu, S. Constantinescu, I. Ovejanu, and Zs. Bartos-Elekes. 2010. Automated Georeference of the 1:20 000 Romanian maps Under Lambert-Cholesky (1916-1959) Projection System. *Acta Geodaetica et Geophysica Hungarica*, Vol. 45, 1, 105-111.
- Satirapod, C., I. Trisirisatayawong, and P. Homniam. 2003. Establishing Ground Control Points for High-resolution Satellite Imagery using GPS Precise Point Positioning. *IEEE International Symposium on Geoscience and Remote Sensing (IGARSS)*. Vols. 1-7, 4486-4488.
- Scardozzi, G. 2009. The Contribution of High Resolution Satellite Images to the Production of Base-maps and Cartographies for Archaeological Research in Turkey and Iraq. *Proceedings of the SPIE - The International Society for Optical Engineering*, Vol. 7478, 74780B.
- Seler, Eduard. 1908. *Die Ruinen von La Quemada im Statte Zacatecas*. In: *Gesammelte Abhandlungen zur Amerikanischen Sprachund Alterthumskunde*, Berlin, Vol. 3.
- Shaker, A., W. Shi, and H Barakat. 2005. Assessment of the Rectification Accuracy of IKONOS Imagery Based on Two-dimensional Models. *International Journal of Remote Sensing*, Vol. 26, 4, 719-731.
- Smith, D.P. and S.F. Atkinson. 2001. Accuracy of Rectification Using Topographic Map versus GPS Ground Control Points. *Photogrammetric Engineering & Remote Sensing*, Vol. 67, 5, 565-570.
- Tamayo, Jorge and R.C. West. 1964. *The Hydrography of Middle America*. In: R. Wauchope (Ed.), *Handbook of Middle American Indians*. University of Texas Press, Austin, Vol. 11, 84-121.
- Timár, G. and C. J. Mugnier. 2010. Rectification of the Romanian 1:75 000 Map Series, Prior to World War I. *Acta Geodaetica et Geophysica Hungarica*, Vol. 45, 1, 89-96.

- Trombold, C.D. 1976. Spatial Distribution, Functional Hierarchies and Patterns of Interaction in Prehistoric Communities around La Quemada, Zacatecas, Mexico. *Archaeological Frontiers: Papers on New World High Cultures in Honor of J. Charles Kelley*, 149-182.
- Trombold, C.D. 1978. *The Role of Locational Analysis in the Development of Archaeological Research Strategy*. Southern Illinois University.
- Trombold, C.D. 1985a. Conceptual Innovations in Settlement Pattern Methodology on the Northern Mesoamerican Frontier. In: Folan, W.J. (Ed.), *Contributions to the Archaeology and Ethnohistory of Greater Mesoamerica*. Southern Illinois University Press, Carbondale, 205–239.
- Trombold, C.D. 1985b. A Summary of the Archaeology in the La Quemada Region. In: Foster, M.S., Weigand, P.C. (Eds.), *The Archaeology of West and Northwest Mesoamerica*. Westview Press, Boulder and London, 237–267.
- Trombold, C.D. 1990. A Reconsideration of Chronology for the La-Quemada Portion of the Northern Mesoamerican Frontier. *American Antiquity*, 55, 308-324.
- Trombold, C.D. 1991. Causeways in the Context of Strategic Planning in the La Quemada Region, Zacatecas, Mexico. *Ancient Road Networks and Settlement Hierarchies in the New World*, 145-168.
- Trombold, C.D., J.F. Luhr, T. Hasenaka, and M.D. Glascock. 1993. Chemical Characteristics of Obsidian from Archaeological Sites in Western Mexico and the Tequila Source Area: Implications for Regional and Pan-Regional Interaction within the Northern Mesoamerican Periphery. *Ancient Mesoamerica*, 42, 255-270.
- Trombold, C.D. 2005a. A Population Estimate for the Epiclassic Middle Malpas Valley La Quemada, Zacatecas, Mexico. *Latin American Antiquity*, 163, 235-253.
- Trombold, C.D., and I. Israde-Alcantara. 2005b. Paleoenvironment and Plant Cultivation on Terraces at La Quemada, Zacatecas, Mexico: The Pollen, Phytolith and Diatom Evidence. *Journal of Archaeological Science*, 323, 341-353.

- United States Geological Survey (USGS). 2012. The Universal Transverse Mercator (UTM) Grid. Retrieved July 1st, 2012 from <http://egsc.usgs.gov/isb/pubs/factsheets/fs07701.html>
- Ward, C. 2005. Using Polynomial Approximation to Rectify Distorted Images. Proceedings of the IASTED International Conference on Modeling and Simulation. Acta Press, 7-12.
- Wiegand, P.C. 1982. Mining and Mineral Trade in Prehispanic Zacatecas. In: Weigand, P. and G. Gwynne (Ed.), *Mining and Mineral techniques in Ancient Mesoamerica*. Anthropology, 6, 87-134.
- Wells, E.C. 2000. Pottery Production and Microcosmic Organization: The Residential Structure of la Quemada, Zacatecas. *Latin American Antiquity*. Society for American Antiquity, Vol. 11, 1, 21-42.
- Wells, E.C., and B.A. Nelson. 2002. Chemical, Technological, and Social Aspects of Pottery Manufacture in the La Quemada Region Of Northwest Mexico. ACS Symposium Series, 831, 185-198.
- Wilcox, D.R., P.C. Wiegand, J.S. Wood, and J.B. Howard. 2008. Ancient Culture Interplay of the American Southwest in the Mexican Northwest. *Journal of the Southwest*, Vol. 50, 2, 103-206.
- Witschas, S. 2003. Landscape Dynamics and Historic Map Series of Saxony in Recent Spatial Research Projects. Retrieved May 4th, 2012 from [http://www2.ioer.de/recherche/pdf/2003\\_witschas\\_ica\\_landscapedynamics.pdf](http://www2.ioer.de/recherche/pdf/2003_witschas_ica_landscapedynamics.pdf)

## VITA

Ryan Thomas Schuermann was born in St. Louis Missouri on April 16, 1973, the son of Patricia and William Schuermann. After completing his work at Cypress Creek High School, Houston, Texas, in 1991 he entered the University of Texas at Austin. From 1992 to 1993 he attended North Harris-Montgomery Community College. During the following years he was employed as a computer programmer, systems administrator and web developer for various companies in Houston and Austin, Texas. Beginning in 2002, he attended Austin Community College until 2004, upon which he re-entered the University of Texas at Austin under the fresh-start program. He received the degree of Bachelor of Arts from the University of Texas at Austin in 2007. During the following years, he worked as an archaeologist for various Cultural Resource Management companies in Austin, Texas. In the fall of 2010, he entered the Graduate College of Texas State University-San Marcos.

Permanent Address: [ryster.com@gmail.com](mailto:ryster.com@gmail.com)

This thesis was typed by Ryan T. Schuermann.